Eyob Simanesew Wesene

Hydraulic modeling using image-derived bathymetry

July 2022

Master's thesis

2022

Eyob Simanesew Wesene

NTNU
Norwegian University of
Science and Technology
Faculty of Engineering
Department of Civil and Environmental Engineering

Master's thesis

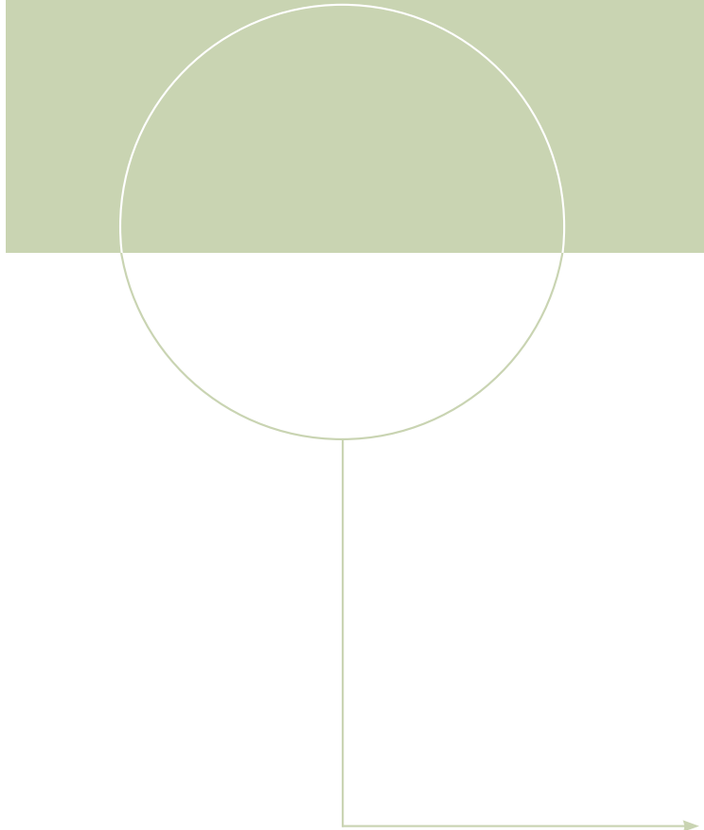

NTNU
Norwegian University of
Science and Technology

NTNU
Norwegian University of
Science and Technology

NTNU
Norwegian University of
Science and Technology

Hydraulic modeling using image-derived bathymetry

Eyob Simanesew Wesene

Master's thesis
Submission date: July 2022
Supervisor: Knut Alfredsen
Co-supervisor: Mahmoud Awadallah

Norwegian University of Science and Technology
Department of Civil and Environmental Engineering

NTNU
Norwegian University of
Science and Technology

Faculty of Engineering
Science and Technology
Department of Hydraulic and
Environmental Engineering

M.Sc. THESIS IN HYDROPOWER DEVELOPMENT

Candidate: **Eyob Simanesew**

Title: **Hydraulic modelling using image-derived bathymetry.**

1 BACKGROUND

River bathymetry is crucial for numerical modelling of flow and other processes in rivers. In recent years bathymetric LiDAR has shown the potential we have for modelling when accurate bathymetry is available. Bathymetry data from aerial campaigns is an expensive method of data collection and might not be feasible for all rivers. Norway and several other countries have a very good covered with topographic LiDAR, but since these datasets do not provide subsurface geometry and is therefore not suitable for hydraulic modelling.

A regional method for deriving bathymetry has been made developed by Håkon Sundt as a part of a PhD study (Sundt et al., Remote Sensing 13, 3897. https://doi.org/10.3390/rs13193897). This method uses imagery from planes or satellites to derive bathymetry based on ratios of RGB bands in the images. The purpose is to test this method for a river where results can be compared with data from topographic LiDAR.

2 MAIN QUESTIONS FOR THE THESIS

The thesis shall cover, though not necessarily be limited to the main tasks listed below. The following main steps will be carried out during the thesis work:

1. Review literature on image-derived bathymetry and the paper by Sundt et al. in particular.

2. Build a bathymetry model for a selected river by combining image data (aerial images) and topographic LiDAR and compare the result with the bathymetric model from green LiDAR data.

3. Evaluate the results from 2) and consider if recalibration of the image method is needed. If the latter is the case, adjust factors and test the new geometry.

4. A hydraulic model should be prepared for the bathymetry from 2/3) and the LiDAR bathymetry for the same river. Calibration should be undertaken, and results compared for the simulation of floods, normal flows, and low flow simulations. Errors should be quantified and causes of errors investigated.

3 SUPERVISION, DATA AND INFORMATION INPUT

Professor Knut Alfredsen and will be the main supervisor for the work. Research assistant Mahmoud Awadallah will co-supervise on hydraulic modelling.

Discussion with and input from colleagues and other research or engineering staff at NTNU, SINTEF, power companies or consultants are recommended. Significant inputs from others shall, however, be referenced in a convenient manner.

The research and engineering work carried out by the candidate in connection with this thesis shall remain within an educational context. The candidate and the supervisors are therefore free to introduce assumptions and limitations, which may be considered unrealistic or inappropriate in a contract research or a professional engineering context.

4 REPORT FORMAT AND REFERENCE STATEMENT

The thesis report shall be in the format A4. It shall be typed by a word processor and figures, tables, photos etc. shall be of good report quality. The report shall include a summary, a table of content, a list of literature formatted according to a common standard and other relevant references. A signed statement where the candidate states that the presented work is his own and that significant outside input is identified should be included.

The report shall have a professional structure, assuming professional senior engineers (not in teaching or research) and decision-makers as the main target group.

All data and model setups should be compiled, documented and submitted with the thesis.

The thesis shall be submitted no later than 1st of July 2022.

Trondheim 3rd of February 2022

_____

Knut Alfredsen
Professor

Declaration

I herein declare that I, Eyob Simanesew Wesene, am the sole author of the thesis title mentioned.

"Hydraulic modeling using image-derived bathymetry"

which was submitted to the Norwegian University of Science and Technology (NTNU) on July 15, 2022, as part of the requirements for the M.Sc. degree in Hydropower Development.

I have fully referenced the ideas and work of other authors, both published and unpublished.

ACKNOWLEDGEMENTS

Before anything else, I'd like to thank the almighty God and his mother for giving me this opportunity, and allowing me to finish my thesis successfully.

I'd like to thank Professor Knut Alfredsen (NTNU) for his numerous recommendations, guidance, and assistance in completing my thesis. I would also like to thank my co-supervisor Mahmoud Awadallah for his assistance, and Dr. Håkon Sundt's for making available his methods for my thesis work.

I'd like to thank my family for their prayers and support. I would like to thank my friends and fellow students who helped me during the work of my thesis

Finally, my thanks go to the Norwegian Agency for Development Cooperation (NORAD) and the Norwegian University of Science and Technology (NTNU) for covering my living expenses while studying for my master's degree.

Abstract

River bathymetry is crucial for the numerical modeling of floods and other river phenomena. Airborne scanning with LiDAR provides accurate river bathymetry. However, data collection using such an instrument is costly and there is a need for appropriate depth retrieval methods from a good quality areal imagery. In the present study, a Regionalized linear model (introduced by Sundt et al. 2021) was used to retrieve depth for Lærdal river and then compare the resulting depth with the airborne scanning LiDAR measurements. Moreover, the retrieved and observed bathymetry were used to model flood inundation for minimum, normal, and high flood flows.

Our results show that the Regional method provides a good estimation of river depth but with a slight overestimation. A comparison of flood inundation simulations between the Regional method and the airborne scanning LiDAR shows the Regional method provides a good estimate for the considered flood flows in this thesis.

Nomenclature

DEM	Digital Elevation Model
GL	Green LIDAR depth or DEM
RL	Red LIDAR depth or DEM
P_r	Pixel value of red band
P_b	Pixel value of blue band
P_g	Pixel value of green band
X_g	Derived Aerial Image of green band combination
X_b	Derived Aerial Image of blue band combination
G-Local	Green band of Local depth or DEM
B-Local	Blue band of Local depth or DEM
G-Regional	Green band of Regional depth or DEM
B-Regional	Blue band of Regional depth or DEM
XS-Interpolated	Cross-sectional Interpolated depth or DEM

Contents

1 Introduction **1**
- 1.1 Background . . . 1
- 1.2 Litrature review . . . 2
  - 1.2.1 Outline Of The Thesis . . . 3

2 Data Sources and Analysis tool **5**
- 2.1 Lidar and Aerial Imagery . . . 5
- 2.2 Hydraulic models . . . 6
- 2.3 R-studio For Statistical Analysis . . . 6

3 Methods **9**
- 3.1 Local And Regional Method's . . . 10
  - 3.1.1 Local Methods . . . 10
  - 3.1.2 Data Analysis . . . 12
  - 3.1.3 Regional Methods . . . 14
- 3.2 LiDAR Data . . . 15
- 3.3 Hydraulic Simulation . . . 16
  - 3.3.1 Inundation Between Observed and Calculated Model . . . 17

4 Results **19**
- 4.1 Local Methods . . . 19
  - 4.1.1 Correlation between Green-LiDAR and Band combination depths . . . 19
  - 4.1.2 Localization . . . 20
  - 4.1.3 Comparison between Local method and Green-LiDAR . . . 22
- 4.2 Regional method . . . 26
  - 4.2.1 The comparison between Regional method and Green-LiDAR 26
  - 4.2.2 Residual raster difference . . . 29
- 4.3 Comparison between XS-Interpolated and G-Regional depth . . . 31
- 4.4 Brightness Adjustment . . . 32
- 4.5 Comparison between Regional and Local Methods . . . 32
- 4.6 Comparison between predicted and observed data . . . 33
  - 4.6.1 River center line comparison between G-Regional and Green-LiDAR. . . . 33

4.6.2 Cross-sectional comparison between all models and LiDAR data from a river 34
4.6.3 Terrain profile for Local, Regional and LiDAR Data. 37
4.7 Hydraulic Simulation for Predicted and Lidar models 38
4.7.1 Minimum flood 38
4.7.2 Normal flood 38
4.7.3 High flood 38

5 Conclusion and Future Work **41**
5.1 Conclusion 41
5.2 Future Works 41

Bibliography **43**

A Methods **45**

B Result **47**
B.1 Cross-sections and correlation coefficient values 47
B.2 Inundation of QM for predicted and Lidar models 47

Figures

1.1 Lærdal river. Location of the study area is shown 1

2.1 Green and Red LIDAR cross sectional view 6

3.1 Flow chart of methods used for retrieving river bathymetry from Aerial imagery and hydraulic simulation. 9
3.2 ISO Cluster to classify the water covered area 11
3.3 Full raster point(Left panel) and cross-sectional point line(right panel) along the river 12
3.4 Four polygons throughout the river reach with five models 13
3.5 XS-Interpolated DEM and interpolated cross sections throughout the river reach 15
3.6 LIDAR Terrain models in Hec-RAS 16
3.7 Hydraulic geometry for flood simulation 17

4.1 Correlation between Derived Areal Image Depth and Green-LiDAR for G-band and B-band combination. Four sections along the river were selected for the present study(see figure 3.4) 20
4.2 Band raster of Green band (left panel) and Blue band (right panel) 21
4.3 Comparison between Local method and Green-LiDAR for different polygon section along the river (see figure 3.4) the comparison define in the x-axis GL- depth (Green-LiDAR depth and in the y-axis G-Local and B-Local depth (Green and Blue color of RGB-band combination) and depth is defined in meter(m). 23
4.4 The comparison that polynomial fitted from section 4(see figure 3.4) 24
4.5 Local method: Comparison between observed and predicted data for merged sections and for the whole river (see figure 3.4) 25
4.6 Comparison between Regional Depth and GL-Depth for different polygon section along the river (see figure 3.4) 26
4.7 Polynomial functions are used to compare the GL-depth and the Regional depth in the fourth section of the polygon. Dimensions are given in meters 27
4.8 Comparison between observed and predicted data for merged sections and for the whole river. 28

4.9 Residual raster: The differences between G-Regional depth and GL-depth in the raster generated by ArcGIS Pro. 29
4.10 The Areal Imagery of the river edge that covered by shadow and dark stones along the river bank. River edge with black stones and fluvial deposit (left panel). River edge with plant shadows (right panel) 31
4.11 The sample distribution of the Residual raster for the considered river area. 32
4.12 The residual raster Set Null. This describes the values between -0.2 and + 0.2 to see how much of the area is between these values. 33
4.13 Comparison between Green band of Regional Depth and XS-Interpolated 34
4.14 Comparison between Local and Regional methods for the green band 35
4.15 Comparison of G-Regional and Green-LiDAR along and across Leardal river. (A) Comparison between G-Regional and Green-LiDAR depths along the center line of the river(ArcGiS). (B) G-Regional and Green-LiDAR Elevations along the center line of the river(HEC RAS) 36
4.16 A comparison of the cross-sections of all of the derived Models with the Green and Red LiDAR data. The terrain profile of section 4 is taken toward to the sea and deeper than other sections. 37
4.17 The extent of the flood inundation is displayed in ArcGIS after a QM flood simulation using HEC-RAS. 39
4.18 The Q200-years flood simulation by HEC-RAS. The extent of the flood inundation for Green Lidar (upper panel) and for predicted and Red Lidar (lower panel). 40

A.1 Extracting point value from raster model as *.dbf file* using GiS-system 45

B.1 Terrain profiles for Local and Regional models, as well at Red and LiDAR data. 47
B.2 Following a QM flood simulation with HEC-RAS, the comparison between G-Regional and Green LiDAR model using flood inundation. The G-Regional model has good fit with GL-model inundation. 49
B.3 QM flood simulation with HEC-RAS, the extent of the flood inundation comparison between RED AND GREEN LiDAR MODEL. RED LiDAR inundates more flood plain area. 49
B.4 Q200-year flood simulation using HEC-RAS, The extent of the flood's inundation for all predicted and Red LiDAR model. 50

Tables

2.1 Point Cloud Platforms used for retrieving bathymetry 5
2.2 Design Floods 7

3.1 Regional Coefficient calculated by Sundt et al. 2021 14

4.1 RGB-Band Coefficient for blue and green band, and number of samples for each sections, all sections combined and for the full raster 21
4.2 Regression coefficients for the Local method. The values were calculated based on corrected and averaged coefficients of the four sections given in table 4.1 22
4.3 Correlation coefficients of calculated by comparing the depth from Local method (Blue and Green color of RGB-band combinations) and the depth form GL-Depth (Green-LiDAR depth) that collected form differnt polygon section along the river (see figure 3.4). 24
4.4 Band ratio coefficients, correlation coefficients and number of samples for each polygon section, for combined four polygons, and for the whole river. 28
4.5 The comparison of the XS-Interpolated and G-Regional depth of coefficients 35
4.6 Comparison between Local and Regional methods for the green band 36
4.7 Normalized Error between predicted and Lidar models 39

B.1 The correlation of different image combinations and methods are displayed with coefficient's with regression fit R^2 and number of samples 48

Chapter 1

Introduction

1.1 Background

The Lærdal river is located on the south side of the Sognefjorden in the municipality of Vestland county in western Norway. The present study focuses on the lower part of the river (see figure 1.1). The study considers flood scenario where a large flood event has occurred (Langsholt et al. 2015). The peak discharge for Lærdal is 800 m^3/s for a flood that occurs once in 200 years, whereas the average discharge is 34 $m3/s$ (Holmqvist 2000).

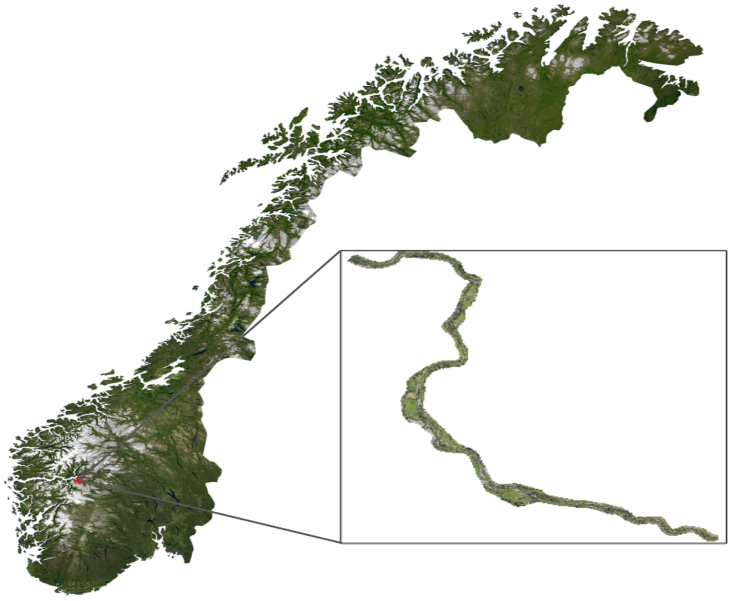

Figure 1.1: Lærdal river. Location of the study area is shown

The main goal of the present study is to retrieve the river's bathymetry along the 13.5 kilometer length of the river by combining data from topographic LiDAR and aerial imagery. The model was constructed utilizing a variety of techniques. A state of the art GIS-Tools, ArcGIS PRO, were utilized during the modeling process. A lin-

ear regression method was used in R-studio to conduct comparison between estimated and ground-truth bathymetry. Four polygon sections along the river were considered for the current study. Different models were evaluated for the reconstruction the bathymetry. After evaluating and selecting the models, the HEC-RAS modeling was used to evaluate how well the models simulates the hydraulic system.

The HEC-RAS Hydraulic modeling was used in the same geometric flow area to simulate for design flood discharge of (QM), 10, 50, and 200 years return period using three derived bathymetry, Red Lidar and Green Lidar bathymetry. The model's normalized error and inundation errors was used to compare inundation with the different bathymetric models.

1.2 Litrature review

River bathymetry is vital for numerical modeling of floods and other river phenomena (Cobby et al. 2001, Mandlburger et al. 2015). In recent years, airborne scanning LiDAR (Green Lidar (GL)) has demonstrated its capability to provide accurate river bathymetry (Guenther et al. 2000). Bathymetry data collection using airborne scanning LiDAR is expensive and might not be feasible for all rivers (Lejot et al. 2007, Kinzel et al. 2013, Alne 2016 and Sundt et al. 2021). According to Breili et al. 2020, about 80% of Norway is covered by the topographic lidar (RL), and the entire country is expected to be mapped by 2023. This topographic LiDAR dataset lacks subsurface geometry. Even though the airborne scanning Lidar provides accurate river bathymetry, only a few rivers were scanned in Norway with such an instrument. In connection with flood inundation, only a few studies were conducted to compare GL and RL. Awadallah et al. 2022 performed numerical modeling of flood inundation using GL and RL terrain models for 11 sites in Norway, and suggested that the RL could lead to high inundation errors even in high flood scenarios. It is thus necessary to perform numerical modeling of flood inundation with a more accurate river bathymetry.

Recently, remote sensing technology (RS) has shown significant advances in mapping river bathymetry (Lyon et al. 1992, Lejot et al. 2007, Marcus et al. 2003 and Winterbottom and Gilvear 1997). Lyzenga 1978 introduced a method for the extraction of river depth from aerial image band combinations. Legleiter, Roberts et al. 2009; were then introduced a more robust method called OBRA (Optimal Band Ratio Analysis) to obtain optimal image band combinations. Legleiter and Harrison 2019; were performed further development of the method and introduced a new version of OBRA that generalizes the calibration process by considering several functional forms for describing the relationship between the image-derived quantity and the flow depth. This relationship depends on factors like ground pixel resolution, substrate color, water column characteristics, and wa-

ter depth itself (Legleiter and Harrison 2019). transferability and application of platform-specific models across rivers. Sundt et al. 2021 studied and tested the use of regionalized linear models for depth retrieval across four Norwegian rivers to provide a potential method for extensive depth mapping in rivers where local bathymetry is lacking.

The availability of bathymetric maps on a national scale could provide a better foundation for river management and flood regulation (Juárez et al. 2021). The main goal of the present study is to

1. Build a bathymetry model for a selected river by combining image data (aerial imgaes) and topographic LiDAR, and compare the result with the bathymetric model from green LiDAR data.

2. Evaluate the results from item 1, and consider if re-calibration of the image method is needed. If the latter is the case, adjust factors and test the new geometry.

3. A hydraulic model should be prepared for the bathymetry from item 1 or 2, and the LiDAR bathymetry for the same river. Calibration should be undertaken, and results compared for the simulation of floods, normal flows, and low flow simulations. Errors should be quantified and causes of errors investigated.

1.2.1 Outline Of The Thesis

Chapter 1 presents a general introduction consisting of background of the study, literature review and problem statement.

Chapter 2 Describes the data source used in the present study and preparation of data.

Chapter 3 describes the methods used in the present study.

Chapter 4 discusses main results of the study.

Chapter 5 summarizes the results, and recommends future work.

Chapter 2

Data Sources and Analysis tool

2.1 Lidar and Aerial Imagery

LIDAR and Aerial imagery data were used for this thesis project. Laerdal river has two Lidars, Green and Red Lidar. The platform is displayed in table 2.1. The Green lidar has the bathymetry data of the river. It is scanned in 2021, and taken from SINTEF as a tiff file. The Red Lidar data have the information of the topographic terrain. It is taken from the national public database from Hoydedata, a national public database, accessed on 10 Feb 2022 as a tiff file Authority 2022. It was broken into different pieces of raster file. The data was been prepared in ArcGIS Pro using the Arc tool *mosaic data*, importing all broken files and merging them into a single tiff file. The region of interest along the Laerdal river can be better defined with the use of polygon. The LIDAR was scanned in 2014, under the name Sogdal2014 as a raster file.

The Aerial imagery data of the Laerdal river was scanned in 2021, downloded from *Norge Bilder* from the Norwegian national web. The data was downloaded as a Goetiff, and it is a combination of Red, Green, and Blue color lights as an RGB-band.

Table 2.1: Point Cloud Platforms used for retrieving bathymetry

Platform	Discharge (m3/s)	Resolution m	Operator	Date of Acquisition	Band
GL	**24**	**0.35**	**AHM**	**26.Sep.21**	**1**
RL	**14**	**0.5**	**Terra Tec**	**18.Dec.20**	**1**
Aerial Imagery	**19**	**0.25**	**Terra Tec**	**21.July.21**	**3**

The Green Lidar Data was already presented as a tiff file. However, the file only consists of the river bank. To include the terrain around the river , a command in Hec-Ras was used, *Add New Teerain*. It was achieved by first importing the Green Lidar, followed by adding the Red Lidar; thereupon merging the terrain data from Red Lidar, and bathymetry of the river from Green Lidar as shown in figure 2.1.

The newly merged file was then Imported into ArcGIS Pro for further work.

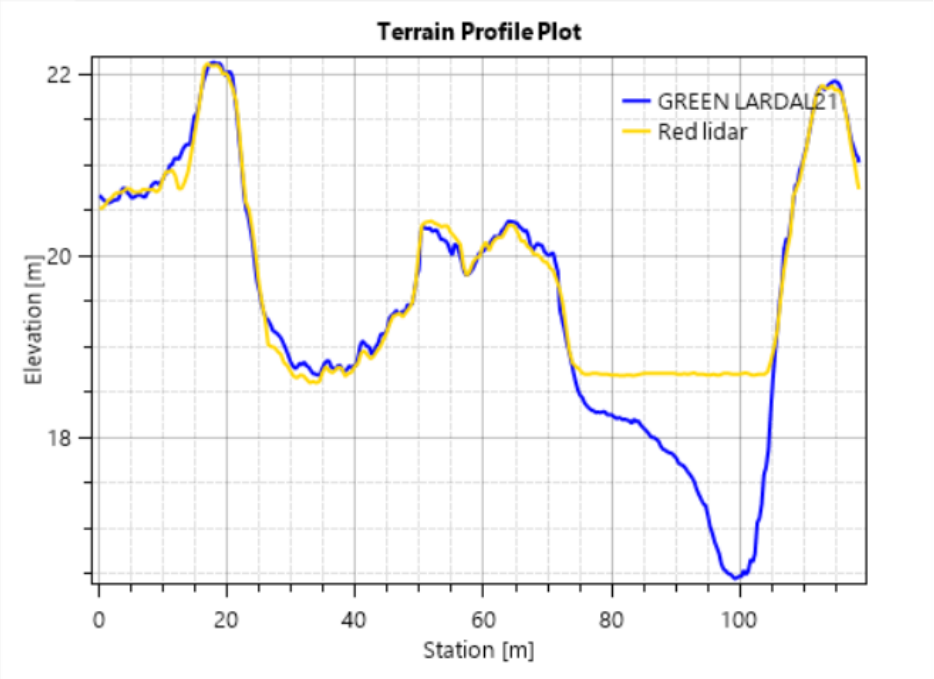

Figure 2.1: Green and Red LIDAR cross sectional view

2.2 Hydraulic models

The calculated and LIDAR model was tested using Hydraulic Simulation in Hec-RAS, by evaluating the flood scenario of Lærdal River. The model was tested in case of minimum flow, normal flow, and flood flow.The flow data is prepared by Holmqvist 2000. The flood flow used for inundation check is shown on table 2.2. ArcGIS and HEC-RAS were used to construct the terrain model. For flood simulation, a topographic flood plan obtained from LiDAR data must be incorporated into all predicted models, which is done by integrating the retrieved model with LiDAR data.

2.3 R-studio For Statistical Analysis

R-Studio is used in this thesis to analyze the statistical work, compare different image derived bathymetric data with green lidar data, and to get the relation these two has. For the statistical analysis, we used the package *(ggplot2)*, *(patchwork)*

Table 2.2: Design Floods

Design Floods	Laerdal river	Unit
QM	**270**	**m3/s**
Q10	**380**	**m3/s**
Q50	**570**	**m3/s**
Q200	**800**	**m3/s**

and *(cowplot)*. This helps us to see the graphs smoothed and clear, with fast regression and adequate polynomial model.

The result is produced by using *library(ggplot2)*,*library(patchwork)* and *library(cowplot)* packages for liner and polynomial regression between GL-LIDAR and Calculated models. Whereas *library(tidyr)*,*library(dplyr)* and *library(Metrics)* are used for MAE(Mean Absolute Error) and RMSE(root mean square error).

Chapter 3

Methods

This chapter examines local and regional methods were used for retrieving river bathymetry from aerial photography. It also examines correlation and comparison of retrieved river bathymetry with Green and Red lidar data. In addition, this chapter provides hydraulic modelling under various flood scenario such as: under low, normal, and flood flow conditions to investigate inundation between calculated bathymetry and Lidar data. Framework 3.1 illustrates the flow of the methods.

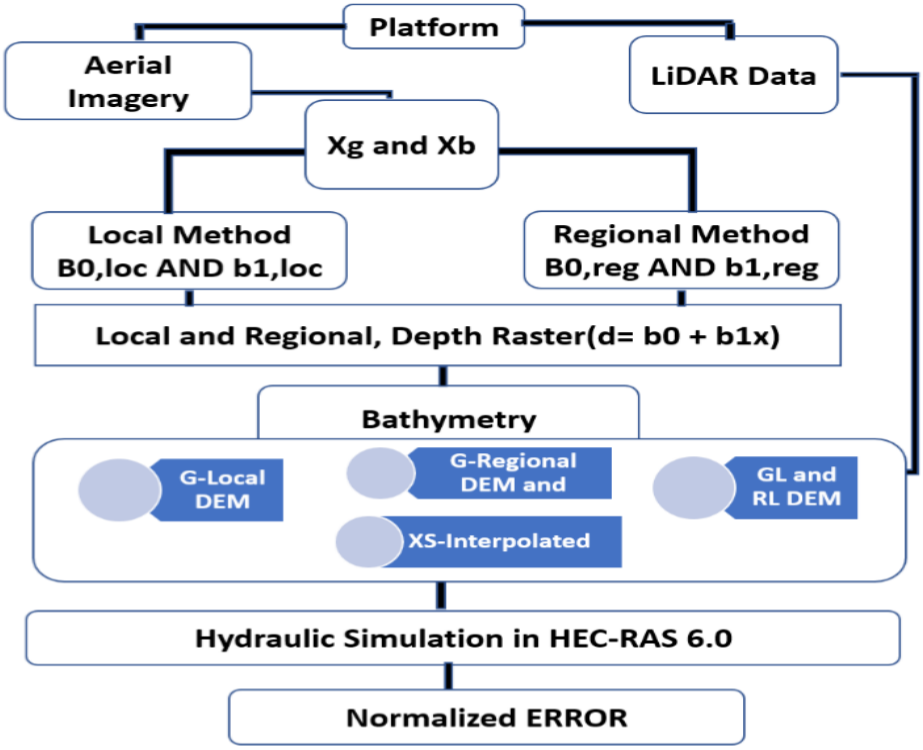

Figure 3.1: Flow chart of methods used for retrieving river bathymetry from Aerial imagery and hydraulic simulation.

3.1 Local And Regional Method's

3.1.1 Local Methods

In this method, we recover locally collected bathymetry using data from aerial imagery. Getting the data ready to use by splitting the image band combinations into Green/Red and Blue/Red image band ratios.

Band Ratio Calculation

The file containing the Aerial Imagery of Lærdal was loaded into the GIS System, and the RGB-band values were extracted. The band colors were then separated according to the band ratios that were established by equations (3.2)and(3.3). In order to calculate the band ratio, the following procedures were carried out in the GIS: The content in the GIS was activated and shown by using the Aerial raster layer in the *Contents pane*. The *Raster Function* in the Imagery tab was then utilized to gain access to the *Band arithmetic* function. The RGB color range is denoted by B1 for Red, B2 for Green and B3 for Blue respectively. Entering the band ratio *B3/B1* (Blue/Red) and *B2/B1* (Green/Red) separately creates two different Band ratio raster files and the red-band is common in this case. The invert icon in the symbology function aids to avoid confusion and to see the difference clearly.

The method described by Sundt et al. 2021 were used to retrieve depth from Aerial Imagery of the RGB-Band (Red, Green and Blue). The depth is given as a function of image pixel value and Ground truth (Eqn. (3.1)):

$$d = b_0 + b_1 X \tag{3.1}$$

where b0 and b1 are respectively the intercept and the slope of the liner relation between Green Lidar Depth (d) and Aerial Imagery of pixels (Legleiter and Harrison 2019), whereas X is a variable that defines logarithmic functions given in

$$X_g = ln(P_g/P_r), \tag{3.2}$$

and

$$X_b = ln(P_b/P_r). \tag{3.3}$$

The variables P_g,P_b and P_r are the RGB-band pixel values of image for Green, Blue and Red respectively, that logarithmic fractions, Green divided Red and Blue divided Red (P is the pixel value, and subscripts b, g, and r represent the band color value). The logarithmic band ratio values are related to the water depth (Stumpf et al. 2003).

Reclass Water Coverd Area

Using band ratio raster file, the area covered by water was classified in order to compute the bathymetry of the river. The calculated band ratio was then inserted as input in *ISO Cluster Unsupervised Classification* tool in the GIS, and the number of classes assigned. The *Re-class* tool differentiates areas with different color of water. Then a single polygon with river edge covered by water is derived from the output raster by using the tool *Raster to Polygon*.

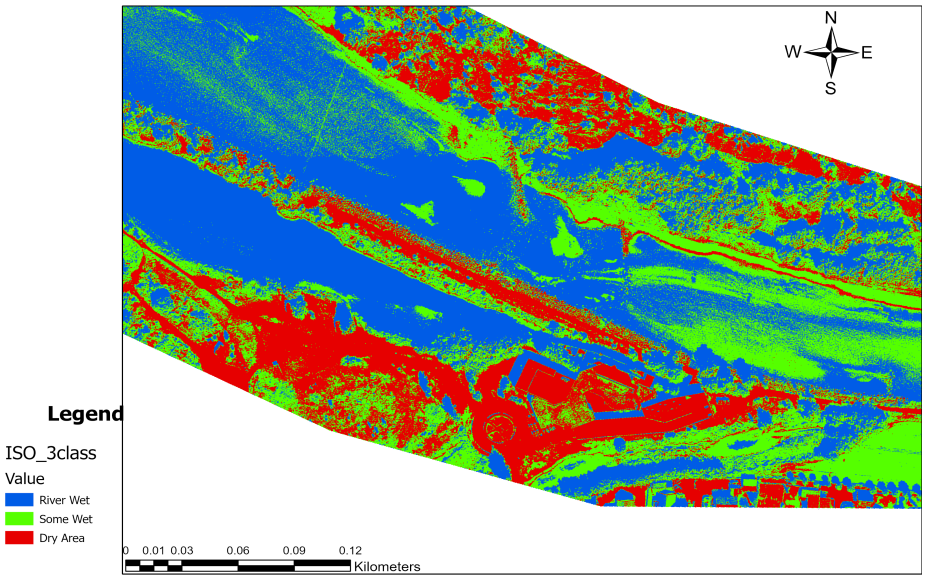

Figure 3.2: ISO Cluster to classify the water covered area

The next step is going in to *Databases* under the function *Catalog* to create a free standing polygon file using the tool *future class*. And then edit the river edge using *re-class file*, which is followed by clipping the water covered area as a raster only using the *Imagery-Raster function* tool in the *Data management*function. Figure 3.2 shows ISO Cluster, which were used to classify the water covered area.

Extract Value of the RGB-Band ratio

The band-ratio of the water covered area is stored as a raster file. Each pixel point value of raster file is calculated in logarithmic function as shown in equations (3.2) and (3.3) using Raster calculator on ArcGIS. Thereon four different Polygon sections were taken thought-out the river reach as shown in figure 3.4, and river cross sections were made within 10 m distance transect along the river center line for the two RGB-Band ratios. Points were then generated along the river cross section line within 5 m distance for each polygon sections, and extract value to

point of corss-sectional lines as shown in the right panel of the figure 3.3. The resulting data were stored as a *.dbf file* which can easily be opened in Excel for post processing. The steps followed in the ArcGIS is given in Appendix A.1.

Figure 3.3: Full raster point(Left panel) and cross-sectional point line(right panel) along the river

Each cloud pixel value of the wet area were converted into points in the GIS by using *Raster to point*. The point features are then stored as *.shp* file. The x-y coordinates were generated for each point in *Attribute table*,the raster point file shown in the left panel of the figure 3.3. Point values for the entire river were extracted using *Extract value to point* and stored as *.dbf* file that can be opened in Excel for post-processing.

3.1.2 Data Analysis

The data sampled, which is the value of band combination, in cross sections and full raster polygon defined area is stored as *.dbf* file. Next the file is opened in Excel, and the Green Lidar depth (GL-depth) is added. This file is then store as *.csv* file to make regression analysis between GL-depth, and Xg- and Xb-band combinations. After the regression analysis, the values are checked and relations with a correlation value < 0.6 are removed and extract the remain. The extracted values will in the following be called corrected coefficients. The average of the corrected coefficients is the localize coefficient's then calculated for each cross-sectional and

polygon-defined along the river. The localize coefficients are then multiplied, followed by adding in liner equation defined as a depth function in equation (3.1). The depth, in this case, is the band combination.The following steps are described by Sundt et al. 2021, with slight adjustments.

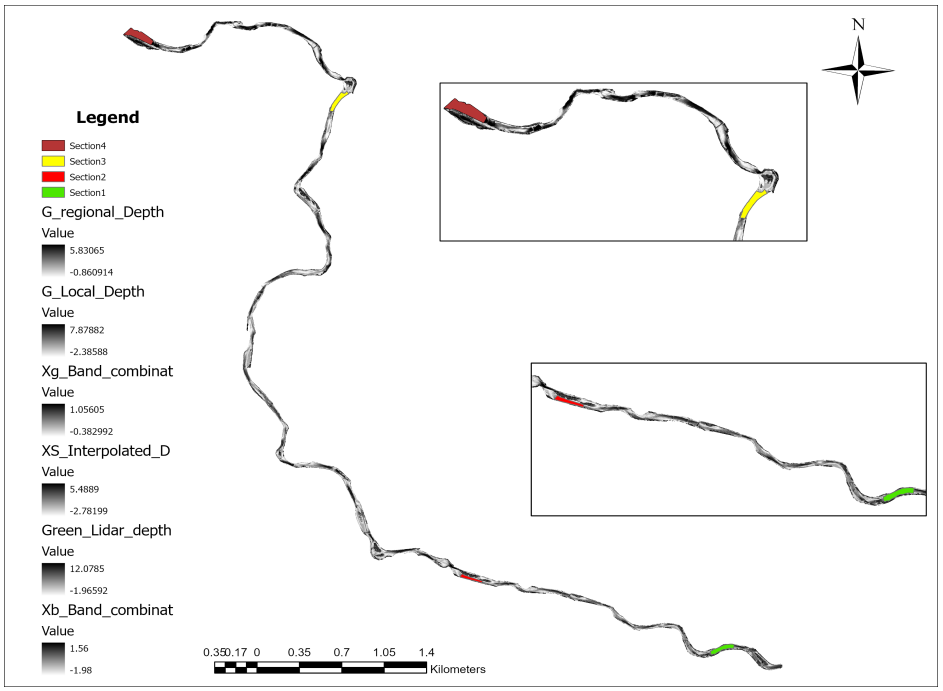

Figure 3.4: Four polygons throughout the river reach with five models

1. We sampled image pixel quantities for the RGB-bands red, green, and blue along with in-situ depth in Numbers of cross-sections for Aerial Imagery in different river polygon section.
2. Using linear regression, we calculated coefficients b_0, dir and b_1, dir for the relationship between Xg, Xb, and GL-Depth, as given in Equations [Green](1)–(3).
3. By assessing the coefficient of determination (R^2) for each cross-section, we removed all cross-sections with an R^2 less than 0.52 to obtain coefficients $b_0, corr$ and $b_1, corr$.
4. Based on the remaining cross-section, we averaged coefficients $b_0, corr$ and $b_1, corr$ for each Polygon sections across the laerdal river reach to obtain a Localize set of coefficients b_0, loc and b_1, loc.
5. In a separate validation polygon thought the river, we applied the models from [B], and [D], to test and assess the model quality.

3.1.3 Regional Methods

Regional methods are introduced by Sundt et al. 2021.He provides regional coefficient values that are dependent on four rivers that are all in the same region: Nea, Gaula, Surna, and Lågen. Regionalized coefficients for the green band and the blue band image combinations are derived from data collected from four rivers. The regionalized slopes and intercepts for Green Band and Blue Band are as defined on the table 3.1. These coefficients are used to calculate regional raster Depth for lærdal river from band Arithmetic previously prepared in section *Band ratio calculation*, as the Aerial Imagery of single band $X_g$and X_b. The *GIS-tool, Raster calculator* is utilized to get the depth raster for Lærdal river using defined slope and intercept, and calculated as shown in equation (3.1); by substituting the value of X_g and X_b on the *X variable*.

Table 3.1: Regional Coefficient calculated by Sundt et al. 2021

	X_b		X_g	
Coefficients	b_0, reg	b_1, reg	b_0, reg	b_1, reg
Regional Value	0.99	2.81	0.92	4.65

$$G-RegionalDepth = b_0, reg + b_1, reg * Xg \tag{3.4}$$

$$B-RegionalDepth = b_0, reg + b_1, reg * Xb \tag{3.5}$$

Where Xg and Xb is the logarithmic fractions of image pixel value of G(Green)-band and B(Blue)-band of Areal Imagery respectively.

XS-Interpolated Depth

The next step is to make a raster out of the G-Regional Terrain cross-section. In HEC-RAS by taking out the numbers of a cross-section along the river, and interpolating the value that has X, Y, and Z as shown in the left side of figure 3.5. This is again interpolated into a new raster terrain as shown on the right side of figure 3.5. The interpolated raster includes only the bathymetry that can merge with RL [1]to get the topography of the terrain. Then the interpolated raster is compared with the G-Regional raster. To create the interpolated bathymetry, the steps are as follows, start by changing the terrain to what we want to interpolate using the tool *Manage layer association* under the tap *Project*. After that, the river line and bank line are created utilizing *rivers* and *bank line* respectively under the tool

[1]RL is the topographic (Red) LiDAR.

Geometry. When creating the river center line, it should be done from upstream to downstream. Whereas there are no criteria for editing the bank line. Along the river center line, the cross-section is auto-generated and defined by the 10 m distance between cross-section lines.

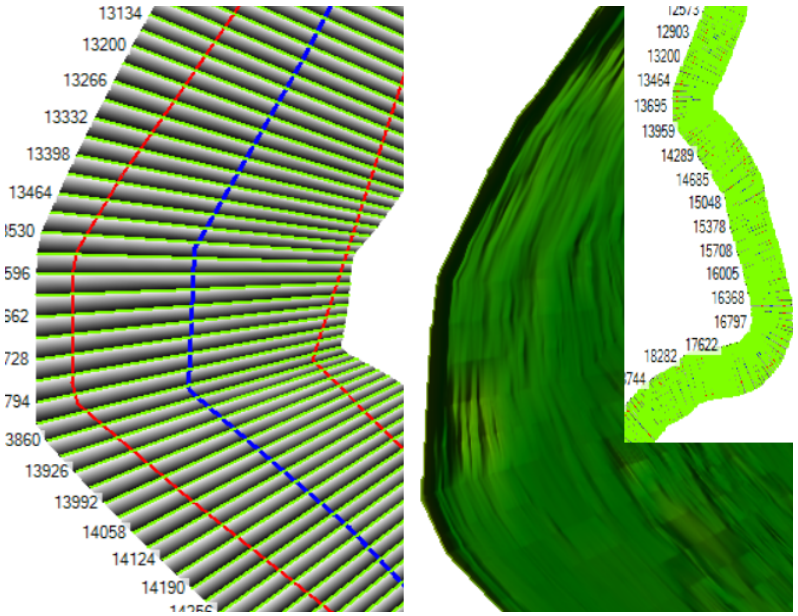

Figure 3.5: XS-Interpolated DEM and interpolated cross sections throughout the river reach

3.2 LiDAR Data

The Green Lidar(GL) is the ground truth[2] of the Laerdal river. The terrain profile is diplayed in figure 3.6. To calculate the depth, GL is subtracted form Red Lidar(RL). The calculation is done using the GIS-tool *Raster calculator* for the computation shown in the equation(3.6). Using the prepared point features shown in figure 3.3, full and cross-sectional points are extracted the value from the Gl depth(d) as raster.

$$d = RL - GL \tag{3.6}$$

[2]ground truth is the bathymetry of river or the riverbed terrain

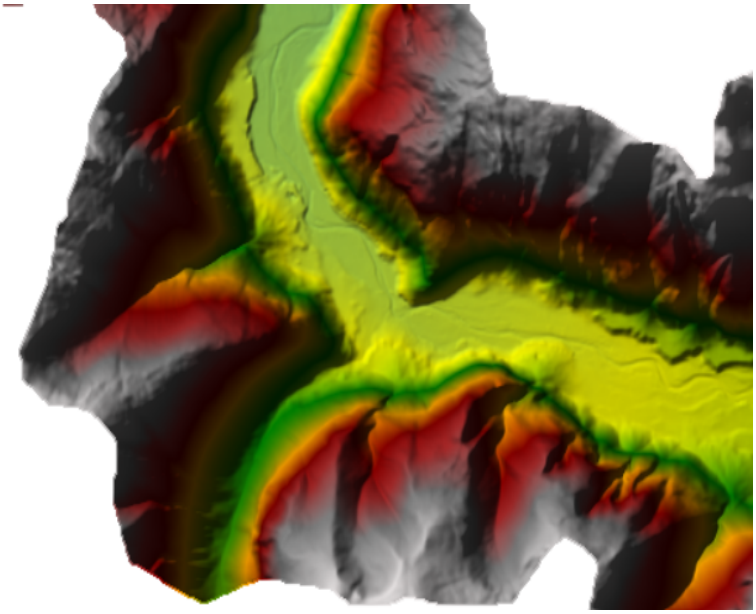

Figure 3.6: LIDAR Terrain models in Hec-RAS

3.3 Hydraulic Simulation

The Hydrologic Engineering Center's (HEC-RAS 6,0) River Analysis System software allows to simulate two-dimensional hydraulic flood inundations. HEC-RAS software was developed by U.S. Army Corps of Engineers and first released to the public in July 1995 (Brunner and Gibson 2005). The Derived depth[3] only illustrate the river flow site without the flood plan. This has a significant influence on the model, since it's without terrain information. when it comes to flood inundation model, different studies focus on the influence of the topographic terrain input (Bures et al. 2019; Cook and Merwade 2009; Reil et al. 2018). The RL (terrain information), Riverbed terrain, calculated depth and GL [4] are merged in HEC-RES using the function *add terrain* listed under the tool *RAS mapper*. The diffusive wave for floodplain flow is represented using St.Venant equation Jung et al. 2012.

The derived DEM (Digital elevation Model) utilizing different methods and the RL are compared against GL. The model differs only in bathymetry, and identical in Terrain. The computational geometry of the river's bathymetry has a grid size of 1x1, while the flood plan has a size of 5x5 as shown in figure 3.7. The downstream boundary condition was set as *normal depth*, and upstream boundary condition as constant *flow hydrograph*, simulated for flood discharge of sixteen hours. The *default Manning's value* for this simulation was 0.03. By running the simulation on GL, the change in the water level is analyzed. The same model with the same

[3]Derived depth the depth based on Local, Regional and XS-interpolated bathymetry
[4]GL is Green LiDAR or that define the bathymetry of the river.

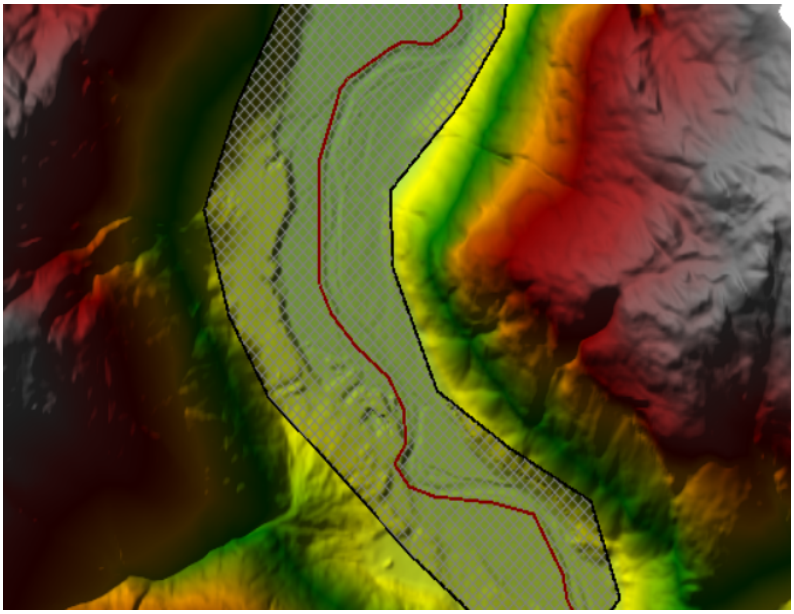

Figure 3.7: Hydraulic geometry for flood simulation

calibration is then tested on RL and derived Models [5]. The simulation is run for minimum, normal, and flood flow, which took ten full days for one Terrain on a *Inter(R) Core(TM) i7-7700 CPU @ 3.60GHz 3.60 GHz* processor.

3.3.1 Inundation Between Observed and Calculated Model

All models that were derived using different methods are tested in different flood-designed simulations using Hec-RAS for minimum, normal, and high flood scenarios. Using the normalized error between observed and predicted models for a certain flood occurrence in particular geometry, this is done by dividing the inundated area predicted by the inundated area observed depending on the inundation of flood extent.

[5]Derived model is the DEM of G-Regional, G-local and XS-Interpolated

Chapter 4

Results

The results include a linear regression analysis of correlation, comparisons of derived bathymetry from two different image processing methods, and a comparison in the ArcGiS-system with various tools. The other method is to compare flood inundation simulated by HEC-RAS in derived bathymetry to flood inundation simulated in observed data of Green-LiDAR (GL) with the same grid geometry.

4.1 Local Methods

4.1.1 Correlation between Green-LiDAR and Band combination depths

The correlation between Green-LiDAR depth (GL-Depth) and band Combination depth is displayed in figure 4.1 for four sections along the river (the four river sections are shown figure 3.4). The RGB-band coefficients and number of samples are given in table 4.1. For section 1 the scatter diagram suggests a weak correspondence between observed data; and band combination with a correlation coefficient of 0.54 for the G-band and 0.05 for the B-band. The G-band shows linear dependence with the Green-LiDAR, however, some of the scatter points biased away from the linear relationship curve. The B-band shows very weak correspondence with Geen Lidar depth.

For sections 2 and 3 (upper right and lower left panel in figure 4.1), the scatter diagrams show very good correlation for the G-band combination with a correlation coefficient of 0.85 and 0.88 respectively. The scatter diagrams for the B-band combination show weak correlation with a correlation coefficient of 0.58 and 0.57 respectively for section 2 and 3. For section 4 the scatter diagram suggests that a polynomial function would best describe the relationship between GL-depth and band combination, despite a good dependence between the variables.

Table 4.1 displays RGB-band coefficients and the number of samples. The variables b0 and b1 are the intercept and the slope of the regression line respectively. While n is the total number of samples taken for the selected polygon section, and for the whole raster contained within the considered river part.

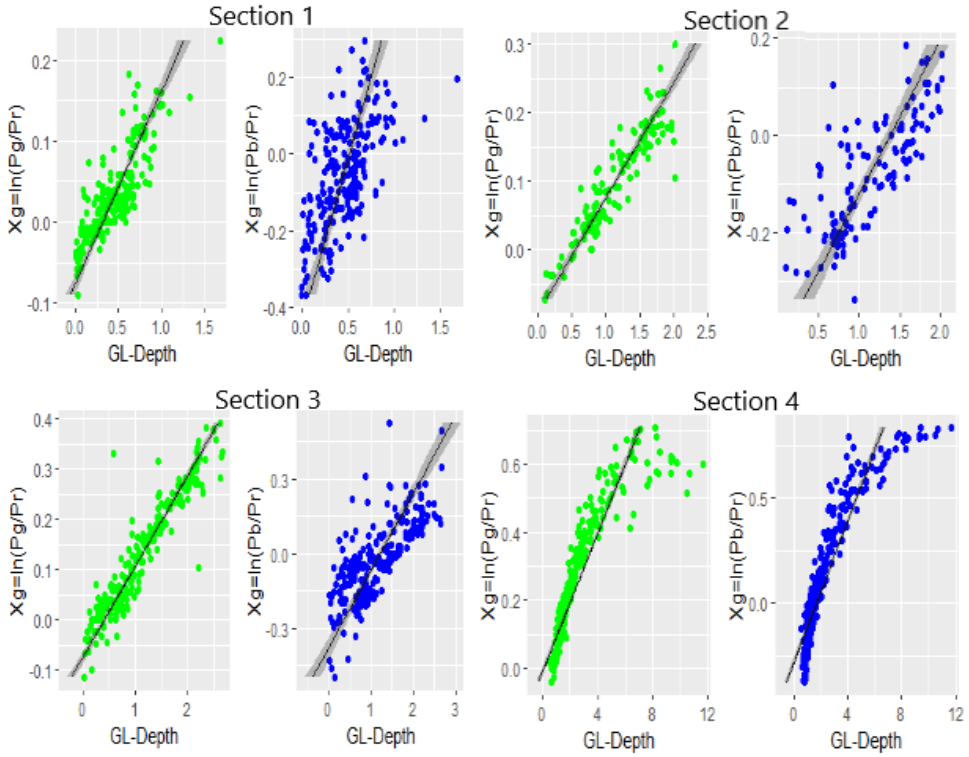

Figure 4.1: Correlation between Derived Areal Image Depth and Green-LiDAR for G-band and B-band combination. Four sections along the river were selected for the present study(see figure 3.4)

The band combination raster is shown in the figure 4.2. The river's edge is well depicted in both Green and Blue bands. In the figure for the G-band, the green foliage along the river's side, an island and the deeper part of the river raster combination are displayed as a darker shade. The B-band is better at defining the river's boundary than the G-band, but it does not provide enough information on the river's depth.

4.1.2 Localization

Localized coefficients were computed based on averages of corrected coefficients for all four sections. To calculate the corrected coefficients for each section, the coefficients b_0 and b_1 in table 4.1 with correlation coefficient (R^2) less than 0.6 were removed. The corrected coefficients for the four sections, denoted by $b_{0,corr}$ and $b_{1,corr}$, were then averaged to estimate the respective coefficients for the localized coefficients (Local method). The the Localized coefficients of the Local method were denoted by $b_{0,loc}$ and $b_{1,loc}$, respectively. This is the average of the coefficients used in the Local method. Before comparing to GL-Depth, samples are

Table 4.1: RGB-Band Coefficient for blue and green band, and number of samples for each sections, all sections combined and for the full raster

	Xb			Xg			
River Secctions	**b0**	**b1**	**R2**	**b0**	**b1**	**R2**	**n**
1	**0.54**	**0.98**	**0.05**	**0.30**	**4.15**	**0.54**	**72**
2	**1.38**	**3.13**	**0.58**	**0.55**	**5.95**	**0.85**	**125**
3	**1.22**	**3.20**	**0.57**	**0.41**	**5.57**	**0.88**	**240**
4	**1.67**	**5.95**	**0.81**	**0.08**	**9.88**	**0.80**	**425**
All sections combined	**1.26**	**5.51**	**0.70**	**0.57**	**7.25**	**0.68**	**1010**
Full raster	**1.02**	**1.56**	**0.19**	**0.64**	**5.22**	**0.57**	**1022050**

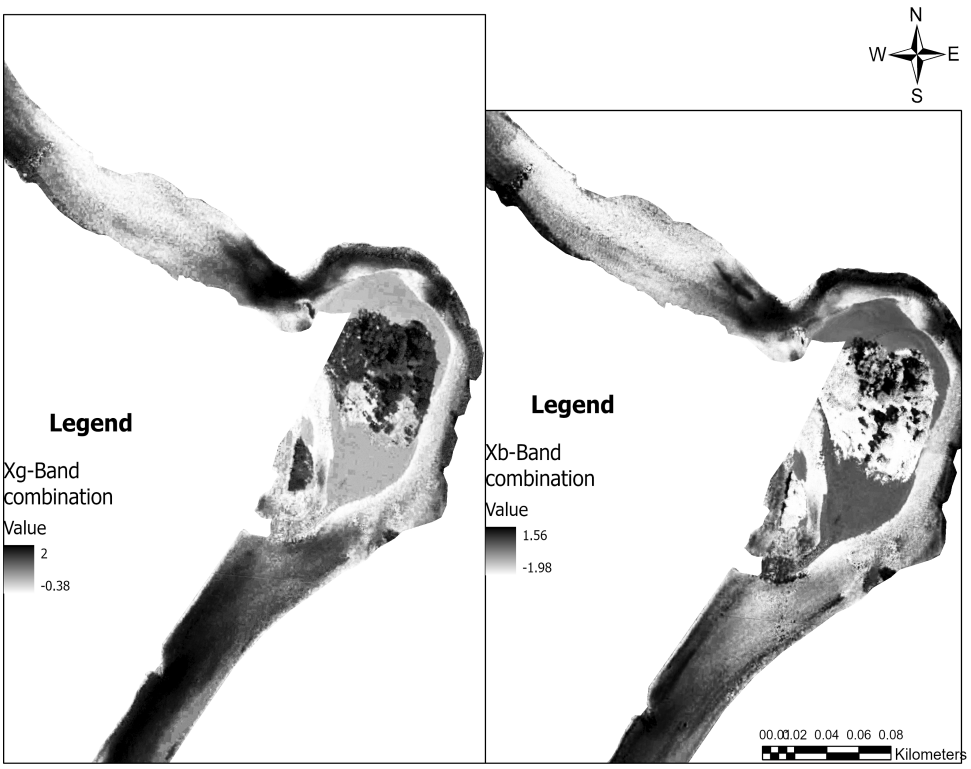

Figure 4.2: Band raster of Green band (left panel) and Blue band (right panel)

collected and the coefficients are displayed on table 4.2. This is done so that the Depth raster can be created using the equation (3.1).

Table 4.2: Regression coefficients for the Local method. The values were calculated based on corrected and averaged coefficients of the four sections given in table 4.1

	Coefficients	
Band-Combination	**b0,loc**	**b1,loc**
Xb	**1.42**	**4.09**
Xg	**0.35**	**7.13**

4.1.3 Comparison between Local method and Green-LiDAR

Figure 4.3 shows comparison between Local method and Green-LiDAR data for various sections along the Lærdal river. The range of out dispersed samples is illustrated by the oblique line (45 degrees) that is established in the scatter plots. Table 4.3 shows observed and predicted regression coefficients, correlation coefficient and number of samples.

Comparison between G-Local depth and GL-depth, for samples in section 1, shows that G-Local provides fairly good prediction with distinct overestimation for depths above 0.5 m. Some of the sample points scattered away from the regression line. The correlation coefficient between G-Local and GL-depth is found to be 0.71. The scatter points are above the 1-1 regression line for depths above 1.0 m.

Comparison between G-Local depth and GL-depth, for samples in sections 2 and 3, shows that G-Local provides a very good estimation of the depth. The correlation coefficients are found to be 0.86 and 0.89 respectively. The G-Local depth and the GL-depth produce a 1-1 regression line, and most of the sample points concentrated around the line. Note that both the regression line and the 1-1 line almost fitted suggesting that the G-Local depth provides very good prediction to the Green-LiDAR depth.

Comparison between G-Local depth and GL-depth, for samples in section 4, shows that G-Local provides a good prediction for depths below 5.0 m. It is observed that the G-Regional gives slight underestimation for depths below 2.0 m and slight overestimation for depths between 2.0 and 5.0 m. The G-Local depths are almost flat for depths above 5.0 m. This is probably due to the difficulty of the band wavelength to penetrate the deeper part of section 4. Note that section 4 is taken from the direction facing toward the sea with river depth reaching up to 12 meters. The correlation coefficient between G-Regional and GL-depth found to be 0.80.

Comparison between B-Local and GL-depth, for section 1, shows that the B-Local provides poor prediction. Sample points are scattered away from the regression line and the samples' regression line deviates significantly from the 1-1 regression

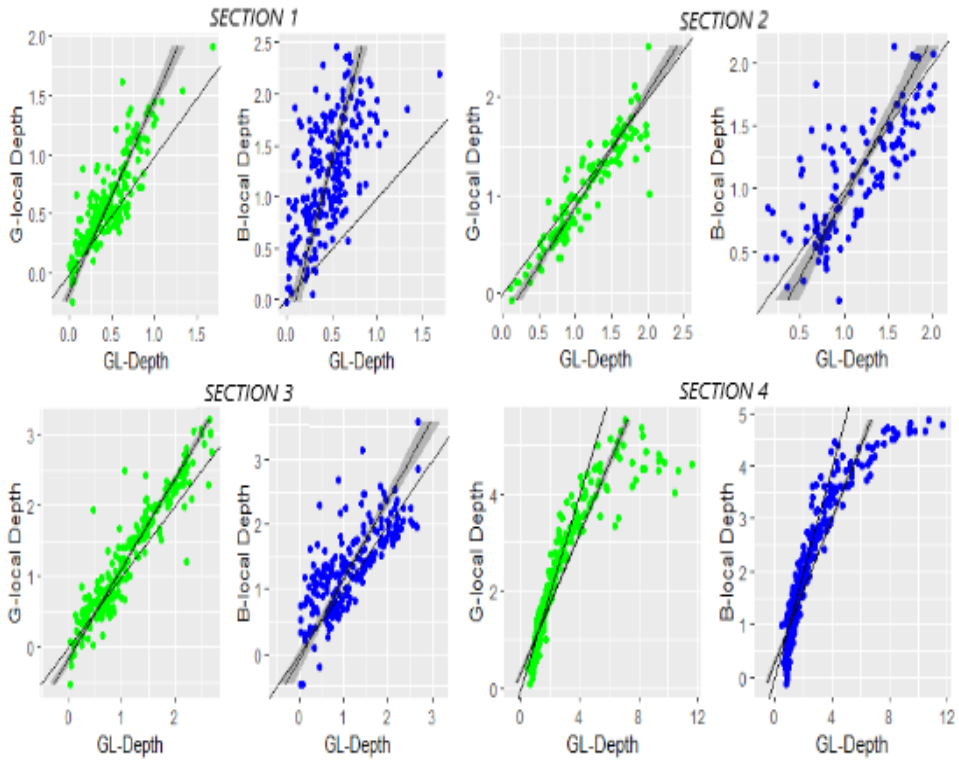

Figure 4.3: Comparison between Local method and Green-LiDAR for different polygon section along the river (see figure 3.4) the comparison define in the x-axis GL- depth (Green-LiDAR depth and in the y-axis G-Local and B-Local depth (Green and Blue color of RGB-band combination) and depth is defined in meter(m).

line. The correlation between B-Local and GL-depth is found to be 0.38.

On the other hand comparison between B-Local and GL-depth shows that B-Local provides a good prediction. The B-Local depth and the GL-depth produce a 1-1 regression line, and sample points are observed to scatter away from the regression line, and this is more pronounced for section 2. The correlation coefficients are found to be 0.58 for both section 2 and 3.

Comparison between B-Local and GL-depth, for section 4, shows that B-Local provides a good prediction for depths below 5.0 m. The B-Local provides slightly better prediction compared to the G-Local with a correlation coefficient of 0.81. The B-Local depths are almost flat for depths above 5.0 m due to the difficulty of the band wavelength to penetrate depths deeper than 5.0 m.

Figure 4.4 shows scatter points of G-Local and B-Local against the GL-depth for section 4 fitted with a polynomial regression. The polynomial regression provides better fit compared to linear regression. The correlation coefficients were increased

Table 4.3: Correlation coefficients of calculated by comparing the depth from Local method (Blue and Green color of RGB-band combinations) and the depth form GL-Depth (Green-LiDAR depth) that collected form differnt polygon section along the river (see figure 3.4).

	B-Local depth			G-Local depth			
River Secctions	**b0**	**b1**	**R2**	**b0**	**b1**	**R2**	**n**
1	O.098	0.30	0.38	0.10	0.61	0.71	213
2	0.27	0.79	0.58	0.26	0.85	0.86	123
3	0.07	0.81	0.58	0.12	0.79	0.89	236
4	-0.40	1.45	0.81	-0.42	1.39	0.80	425
All sections combined	-0.54	1.36	0.72	-0.27	1.26	0.82	1003
Full raster	0.51	0.37	0.16	0.34	0.78	0.57	910987

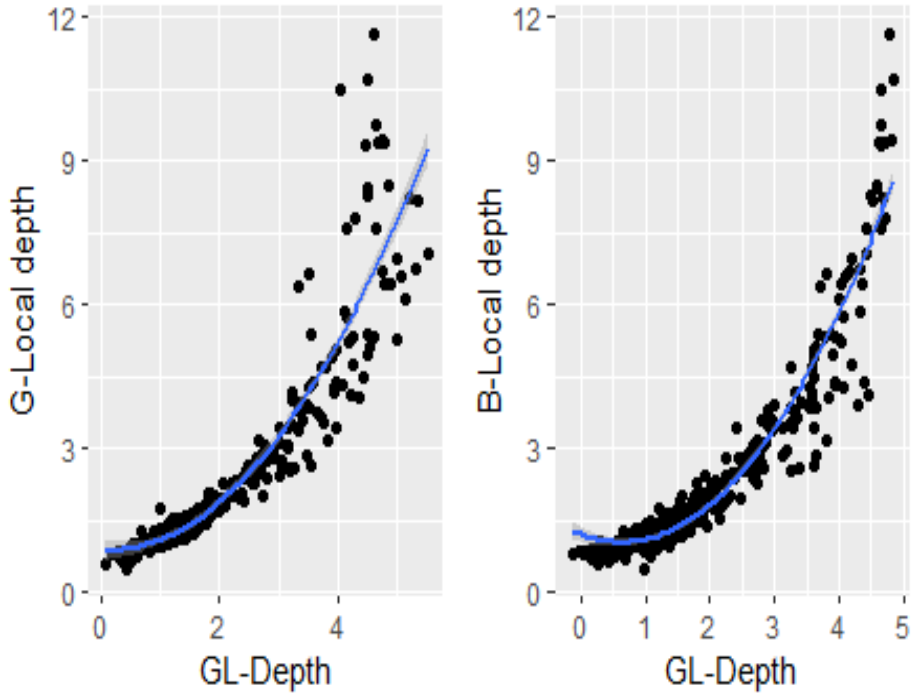

Figure 4.4: The comparison that polynomial fitted from section 4(see figure 3.4)

to 0.86 and 0.92 respectively for B-Local and G-Local. Note that the Local method depths are limited to depths shallower than 5.0 m. This is because the band wavelengths are not able to penetrate the deeper part of section 4.

Figure 4.5 shows comparison between Local method and Green-LiDAR data for

the four sections combined and for the entire raster.

The scatter plots for the combined sections (upper plots) show that the Local method appears to be generally good for both bands and for depths below 5.0 m.Observed depth goes up to 12 m deep for the river section facing to the sea. The correlation coefficients fit B-Local and G-Local are found to be 0.72 and 0.82 respectively.

A comparison between Local method and GL-depth is shown in the lower two scat-

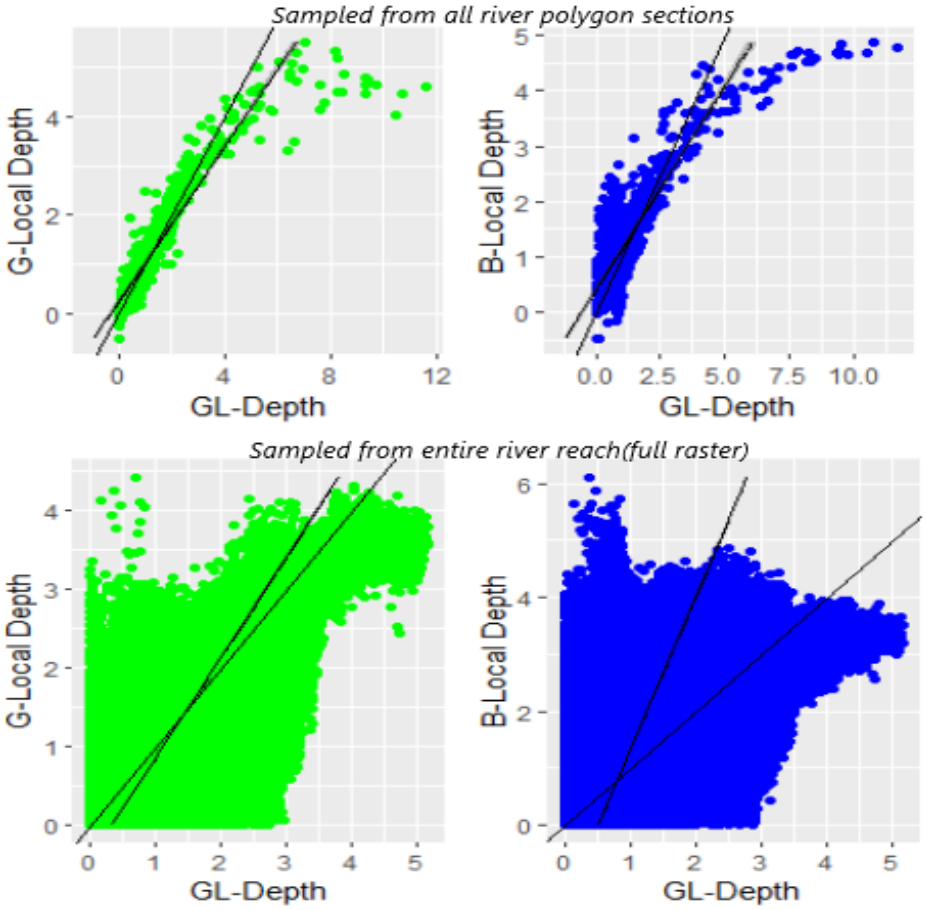

Figure 4.5: Local method: Comparison between observed and predicted data for merged sections and for the whole river (see figure 3.4)

ter plots. The correlation coefficients for G-Local (lower left) and B-Local (lower right) are found to be 0.57 and 0.16. This demonstrates that the B-Local depth was an unreliable predictor of the observed depth, whereas the G-Local depth was a reliable predictor of the observed depth. For G-Local sample points were collected along the 1-1 regression line for B-Local sample points were scattered away from the 1-1 regression line.

4.2 Regional method

4.2.1 The comparison between Regional method and Green-LiDAR

Comparison between Green-LiDAR Depth (GL-Depth), and depth generated by Regional method (REG) is shown in figure 4.6 . The range of dispersed samples is illustrated by the oblique line that is established in the scatter plots. The G-Regional depth shows very good correspondence with GL-depth for all for sections. The correlation between G-Regional and GL-depth is found to be 0.67, 0.85, 0.88 and 0.80 respectively for Sections 1, 2, 3 and 4. It is observed that most of the samples lie inside the 45 degrees line. The correlation coefficient for Section 1 is relatively low, and some of the sample points are scattered away from the linear line. For polygon segment 4 (Section 4), the Regional method provides poor prediction for GL-depth greater than 5 m. This polygon segment is taken from the direction facing toward the sea, hence the GL-depth goes up to 12 meters, while the G-Regional and B-Regional depths are not.

The B-Regional for sections 1-3 provides poor prediction compared to the G-

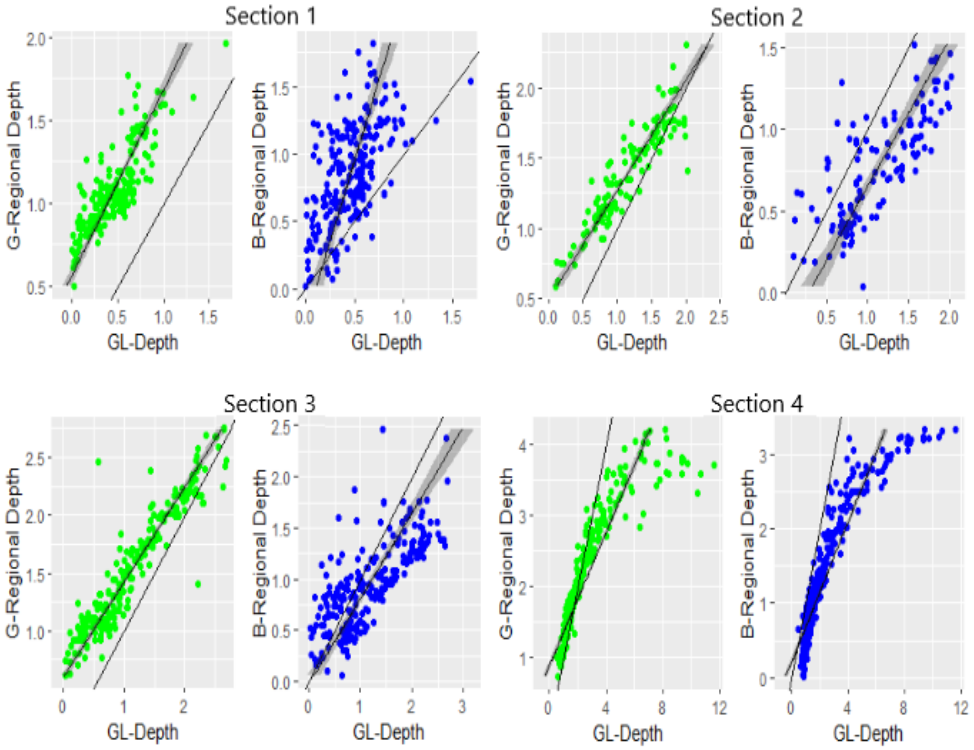

Figure 4.6: Comparison between Regional Depth and GL-Depth for different polygon section along the river (see figure 3.4)

Regional, and sample points are merely scattered away from the linear line.

The scatter plots suggest that the G-Regional overestimates the GL-depth for sec-

tion 1, and underestimates the GL-depth for Sections 2 and 3. A polynomial fit considered to be good to describe the distribution for Section 4 (see figure 4.7). In this case, the polynomial fit has increased the correlation coefficient from 0.83 to 0.86 for G-Regional; and 0.8 to 0.83 for B-Regional depth.

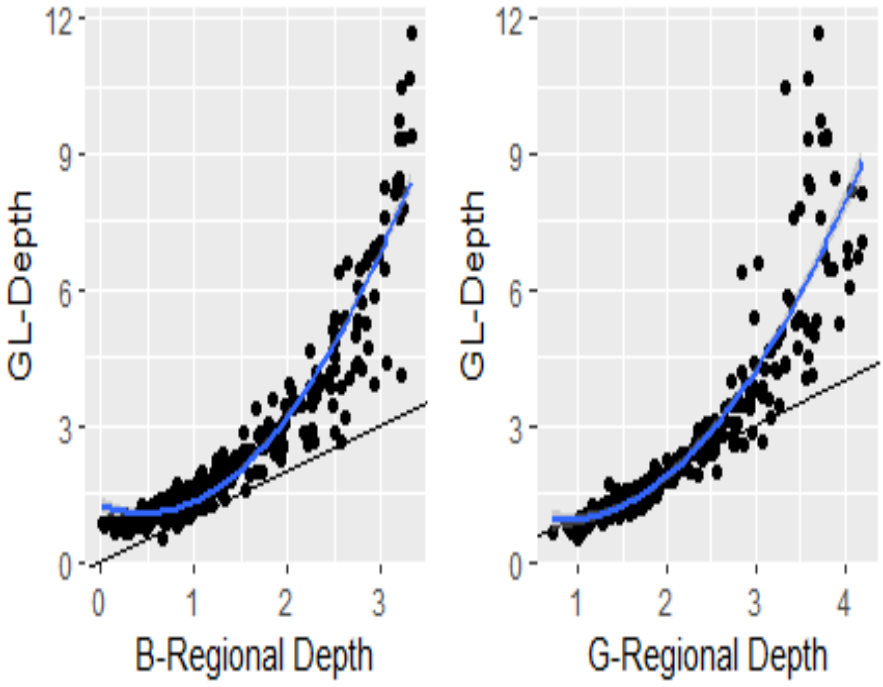

Figure 4.7: Polynomial functions are used to compare the GL-depth and the Regional depth in the fourth section of the polygon. Dimensions are given in meters

The sample points for the present study are shown in figure 4.8 for the entire river (full raster), as well as for the four polygons combined. The maximum depth for the G-Regional of the combined polygons is around 4 m, whereas the maximum depth for the B-Regional is around 3 m (upper two scatter plots). The lower two scatter plots show Regional depth against GL-depth for full raster. The G-Regional compares fairly well with GL-depth whereas B-Regional shows poor comparison. The root-mean-squares-error(RMSE) between G-Regional and GL-depth is found to 0.25. Whereas the mean-absolute-error (MAE)is 0.34. Since section 4 is taken from the direction facing toward the sea it is expected to have increased the error for the combined polygons when a linear regression is assumed. The regression and correlation coefficients and number of samples for each polygon, combined polygons and the whole raster are displayed in table 4.4.

The Regional depth and GL-depth regressions show that the G-Regional depth is

Table 4.4: Band ratio coefficients, correlation coefficients and number of samples for each polygon section, for combined four polygons, and for the whole river.

	G-Regional depth			B-Regional depth			
River Sections	**b0**	**b1**	**R2**	**b0**	**b1**	**R2**	**n**
1	-0.50	0.89	0.67	0.11	0.41	0.35	212
2	-0.63	1.28	0.85	0.27	1.12	0.58	125
3	-0.72	1.21	0.88	0.03	1.19	0.56	236
4	-1.90	2.13	0.80	-0.46	2.14	0.83	422
Combined polygons	-1.62	1.94	0.81	-0.60	1.99	0.72	1001
Full raster	-0.43	1.16	0.58	0.45	0.59	0.19	983264

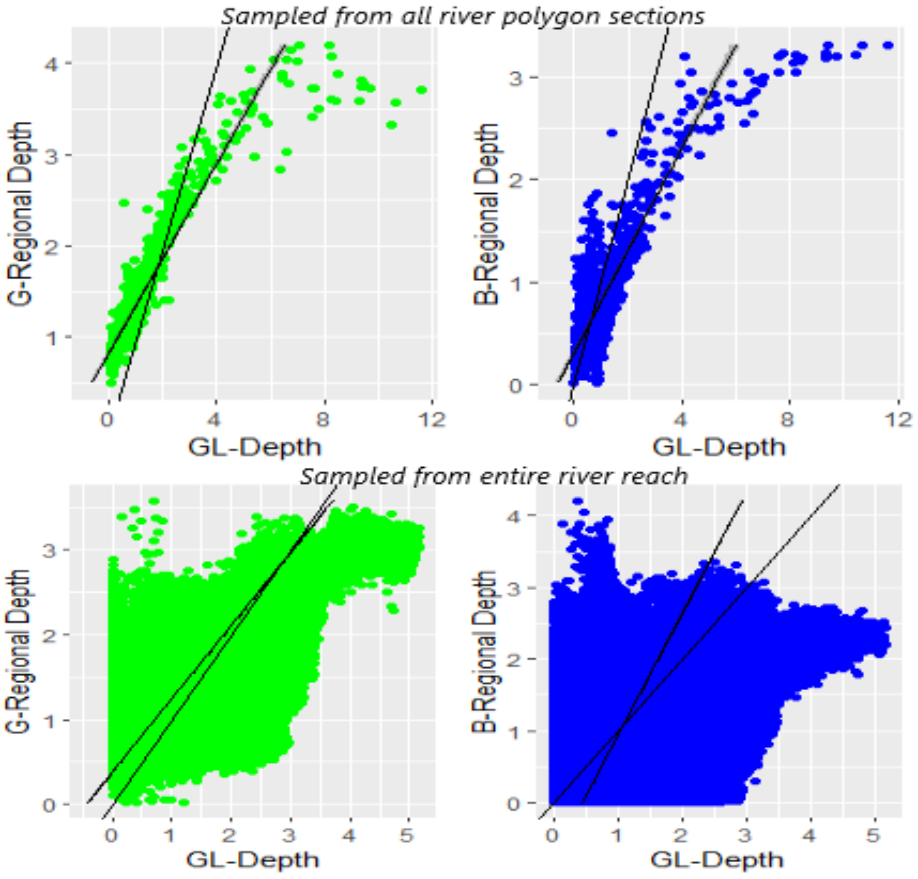

Figure 4.8: Comparison between observed and predicted data for merged sections and for the whole river.

anticipated to be between 2 and 3 meters deep. However, it is estimated to be up to 4 meters deep for a river that is rather shallow. It is anticipated that the B-Regional will be 1.5 meters deep. On the other hand; simulations reveal that it

may go as deep as 3 meters. The wavelengths of rays in the green band are better able to pass through water surface than the blue band.

4.2.2 Residual raster difference

It is difficult to get a complete picture of the difference between GL-Depth and G-Regional depth merely by estimating the regression function. It is thus necessary to generate Digital Elevation Model (DEM) raster for the G-Regional in ArcGIS, and then subtract Green-LiDAR (GL) as shown in equation (4.1),

$$Residual raster = G\text{-}Regional\ DEM - GL\ DEM. \tag{4.1}$$

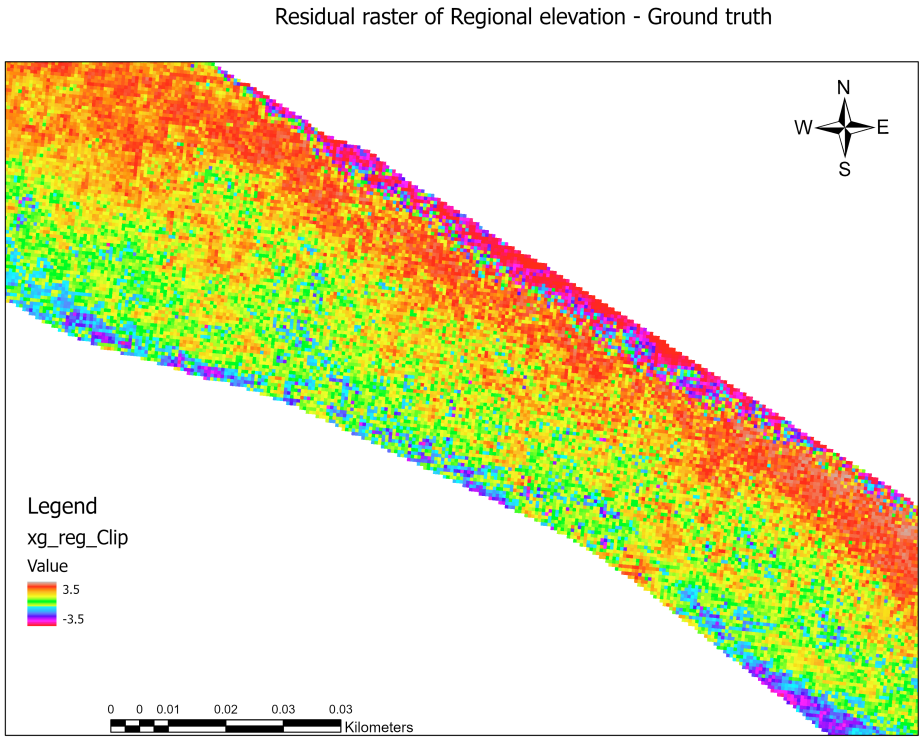

Figure 4.9: Residual raster: The differences between G-Regional depth and GL-depth in the raster generated by ArcGIS Pro.

The difference between G-Regional elevation and GL (residual raster) is shown in figure 4.9. The residual raster is found to be between -3.5 and 3.5. Negative residual raster indicates the G-Regional depth is deeper than the GL-depth. Whereas positive residual raster suggests the GL-depth is deeper than the G-Regional depth.

The red colored area in the residual raster difference indicates that G-Regional method gives depth values deeper than GL. This is clear when one looks at the Aerial picture depicted in figure 4.10. The shadows from the surrounding plants, the dark stones, and the fluvial sediments on the riverbank contribute to false elevation. This is considered as deep river part during the conversion from aerial imagery to band combinations. This has some effect on the accuracy of prediction, and causes aerial images to count river parts as being deeper than they actually are.

It is clear from examining the Orange color in the raster that the bathymetry of the GL extends more below the surface than that of the G-Regional. This is due to the fact that the deeper the bathymetry of the river the darker the river becomes. This makes it more difficult for light to go deeper down the river bottom using RGB-band wavelengths. The G-Regional calculates the the river depth as deep as it is clearer and penetrable by RGB-band wavelengths.

The Green color indicates that the G-Regional depth bathymetry provides precise forecasts for the GL. In this case the difference between the raster is very close to zero.

Figure 4.11 depicts the distribution of the remaining bathymetric elevation difference along the river. Thirty three percent of the remaining disparity between the predicted and observed data is with -0.25 m depth. The observed and predicted elevations are canceled out because 16 percent of the difference is zero. According to the distribution of the sample, which ranges between -0.75 and 0.5, the G-Regional elevation is the most effective method for presenting the ground truth. The majority of the samples in the G-Regional bathymetry are below zero, which indicates that it is shallower than the GL-bathymetry. This means that the G-Regional overestimate the depth of the Lærdal river, but the difference is not significant.

We used symbology to make the necessary adjustments to the residual raster to account for the ±0.2 (see figure 4.12). The value ±0.2 is selected based on visual evaluation of the sample distribution in figure 4.11. The difference in sample values used to determine which sections of the river body are between this point and which are not. Using the previously provided raster and sample distribution (figure 4.11), we can see that 45 percent of the raster sample difference falls within the range of ±0.2. Our investigation, led us to the conclusion that the Regional predictions are plausible.

Figure 4.10: The Areal Imagery of the river edge that covered by shadow and dark stones along the river bank. River edge with black stones and fluvial deposit (left panel). River edge with plant shadows (right panel)

4.3 Comparison between XS-Interpolated and G-Regional depth

The method we tune for the particular river by interpolating the cross-sections in figure 3.5 of the G-Regional DEM would be as effective as the Regional method. This XS-Interpolated depth is obtained using G-Regional bathymetry, which is then interpolated to eliminate sample scatter and smooth the water bed. As indicated in the figure 4.13, we utilize linear function to compare the correlation between the XS-interpolated depth and the G-Regional depth. The four portions of the river are illustrated in (Figure 3.4). The four polygonal portions share no visible distinction. As indicated in table 4.5, there may be minor variances in the correlation coefficients. Even though there is a close connection between the two methods, it is difficult to discern between GL-depth and XS-Interpolated depth.

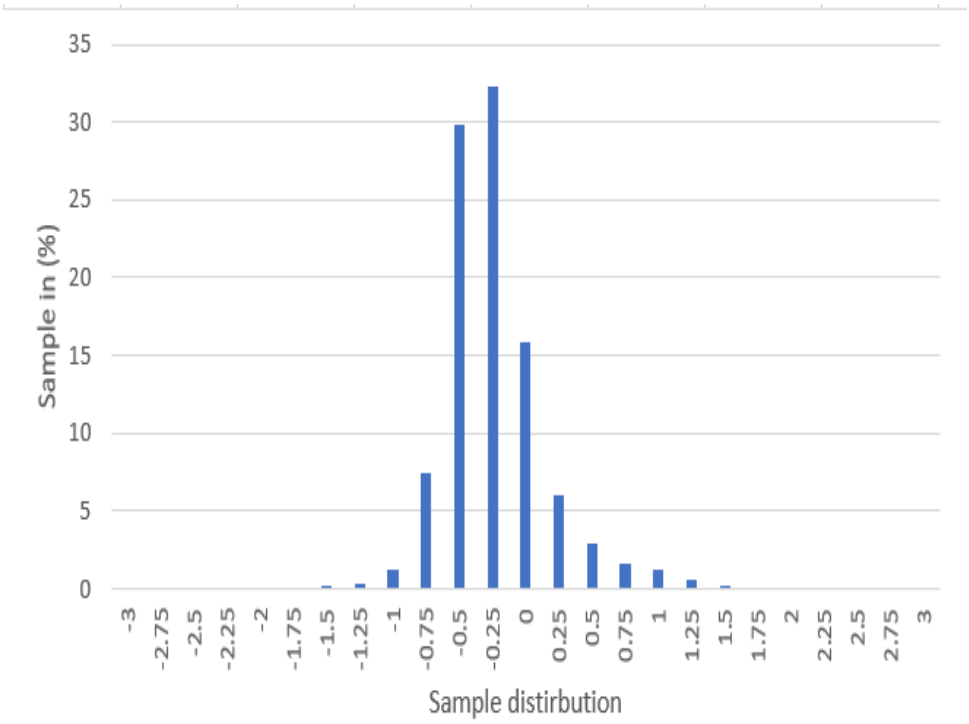

Figure 4.11: The sample distribution of the Residual raster for the considered river area.

4.4 Brightness Adjustment

The brightness of the Lærdal river has not been adjusted since the BR-value is close to one (using equation stated by Sundt et al. 2021). This is because the Lærdal river is brighter and clearer, requiring no brightness adjustment. The results show that the regional method slightly overestimates the ground truth, as does the Local method.

4.5 Comparison between Regional and Local Methods

Comparison between Local and Regional methods with the Green-LiDAR data were discussed in detail in the previous sections. In the present section we discuss how well the two methods able to predict the observed bathymetry. Figure 4.14 shows comparison between Local and Regional methods with the Green-LiDAR bathymetric data for the four sections (see figure 3.4 for the positions of the four sections). Table 4.6 shows correlation coefficients for Local and Regional methods for the green color band. The correlation coefficients for the four sections lies between 0.71 and 0.89.

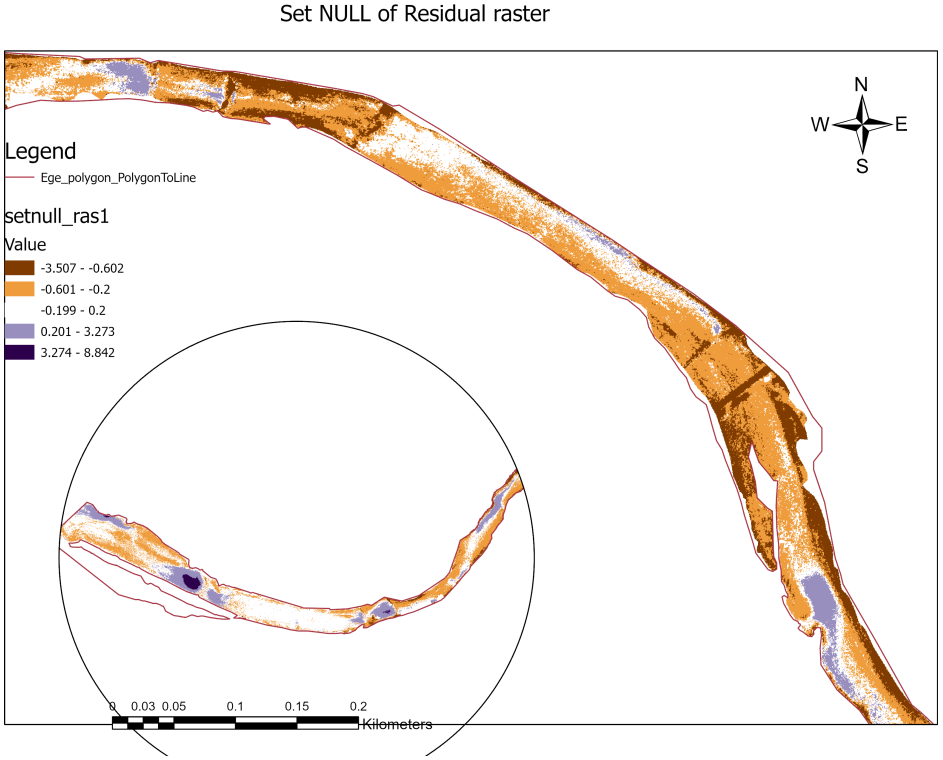

Figure 4.12: The residual raster Set Null. This describes the values between - 0.2 and + 0.2 to see how much of the area is between these values.

The Local method provides better prediction of the bathymetry compared to the Regional method for all of the four sections. For reasons explained in the previous sections, both the Local and the Regional methods were unable to produce the bathymetry for river deeper than 5 m.

For section 1 the Regional method overestimates the bathymetry for all depths. For sections 2 and 3 the method provides a good prediction with visible overestimation of the bathymetry for shallower depths.

4.6 Comparison between predicted and observed data

4.6.1 River center line comparison between G-Regional and Green-LiDAR.

As discussed in the previous sections it is possible to obtain river bathymetry from remote sensing data. Figure 4.15 shows comparison between G-Regional and Green-LiDAR along the Leardal river. The prediction performed by the two meth-

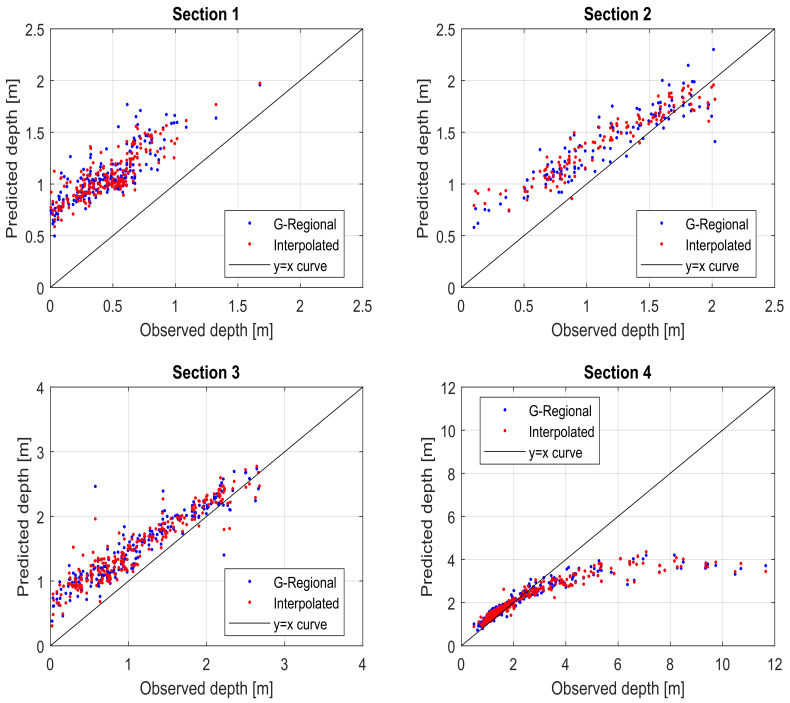

Figure 4.13: Comparison between Green band of Regional Depth and XS-Interpolated

ods is good in general. Comparison between G-regional and GL terrain along the river center-line using HEC-RAS (figure 4.15 B), show that the G-Regional either underestimates or overstates the terrain at several locations along the river axis.

In addition, the ArcGIS was used to compare the G-Regional and Green-LiDAR terrain along the center-line of the Leardal river (figure 4.15 A). The resulting comparison produces a correlation which is equal to one, which is an optimum value for the river center-line. The data was taken along the river at every 10 m interval and it consists of deep and shallow sections of the river.

4.6.2 Cross-sectional comparison between all models and LiDAR data from a river

Throughout the Lærdal River, this graph compares all predicted and LiDAR models. It is essential to notice that all river cross-sections are represented in the sections, as stated in the linear regression comparison, which includes both deep and shallow portions of the river. Appendix B.1 depicts the cross-sections and their respective placements. G-Local bathymetry provides the closest approximation to

Table 4.5: The comparison of the XS-Interpolated and G-Regional depth of coefficients

	G-Regional depth			XS-Interpolated depth			
River Secctions	**b0**	**b1**	**R2**	**b0**	**b1**	**R2**	**n**
1	-0.50	0.89	0.67	-0.62	1.00	0.71	212
2	-0.63	1.28	0.85	-0.84	1.42	0.90	125
3	-0.72	1.21	0.88	-0.73	1.22	0.90	236
4	-1.90	2.13	0.80	-2.16	2.26	0.82	422

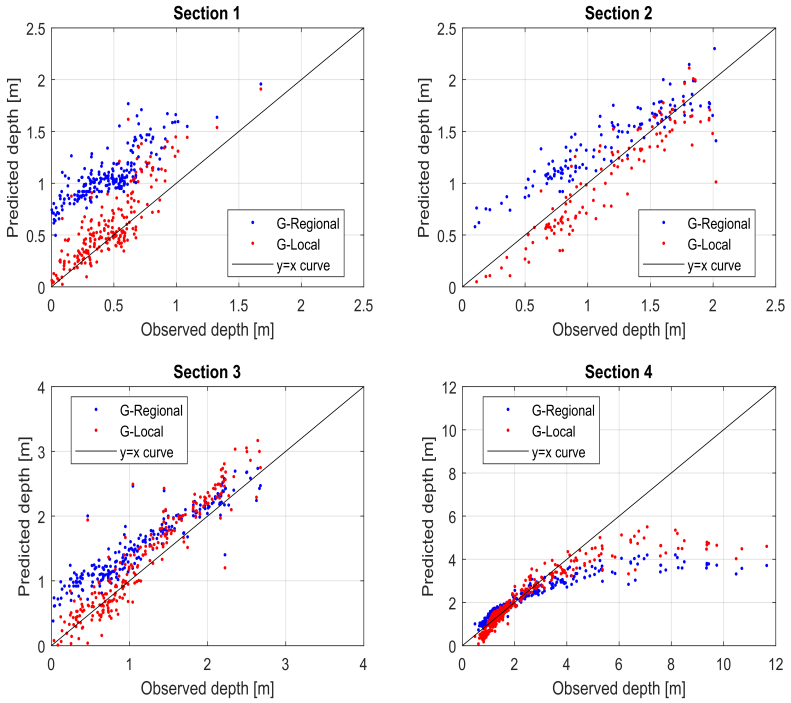

Figure 4.14: Comparison between Local and Regional methods for the green band

Green-LiDAR in all sections, as opposed to G-Regional and XS-Interpolated bathymetry. In this instance, the RL merely displays the river's water level, while other methods generate only bathymetry data; yet, the area's topography is derived from the RL. Consequently, the topography is consistent.
In sections 1-3, the G-Regional and XS-interpolated data coincide, resulting in a reliable GL prediction. The G-Local bathymetry fits GL well and is a substantial advance over the G-Regional and XS-interpolated bathymetric models. In Section 4, the GL depth is up to 12 meters, the G-Local depth is up to 5 meters, and others

Table 4.6: Comparison between Local and Regional methods for the green band

	G-Regional depth			G-Local depth			
River Secctions	**b0**	**b1**	**R2**	**b0**	**b1**	**R2**	**n**
1	-0.50	0.89	0.67	0.10	0.61	0.71	207
2	-0.63	1.28	0.85	0.26	0.85	0.86	123
3	-0.72	1.21	0.88	0.12	0.79	0.89	232
4	-1.90	2.13	0.80	-0.42	1.39	0.80	422
All sections combined	-1.62	1.94	0.81	-0.27	1.26	0.82	1001
Full raster	-0.43	1.16	0.58	0.34	0.78	0.57	920613

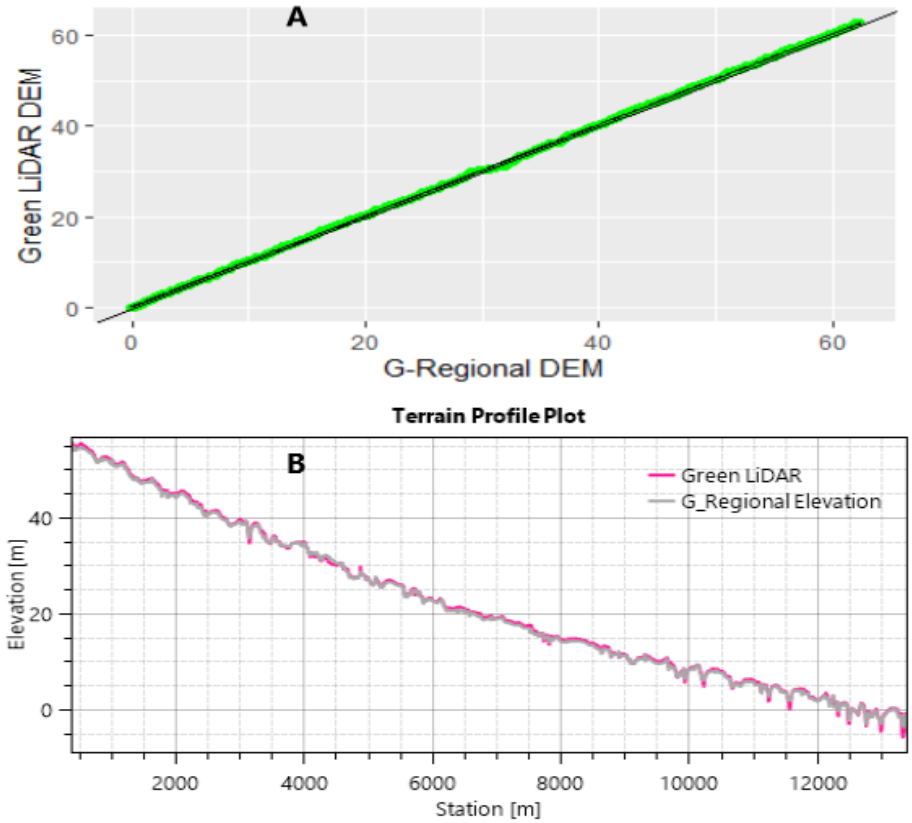

Figure 4.15: Comparison of G-Regional and Green-LiDAR along and across Leardal river. (A) Comparison between G-Regional and Green-LiDAR depths along the center line of the river(ArcGiS). (B) G-Regional and Green-LiDAR Elevations along the center line of the river(HEC RAS)

predict an approximate depth of 4.5 meters. This particular segment was taken in the direction of the ocean.

4.6.3 Terrain profile for Local, Regional and LiDAR Data.

Figure 4.16 shows of river bathymetry profiles at four locations (one from each sections) along the river, for different methods. All the methods provide good prediction to the depth in general. The For terrain profiles taken from section 1, the Regional methods overestimates the observed depths. Whereas the Local method shows provides a good estimate as expected.
For terrain profiles taken from section 2 and 3 both Local and Regional methods

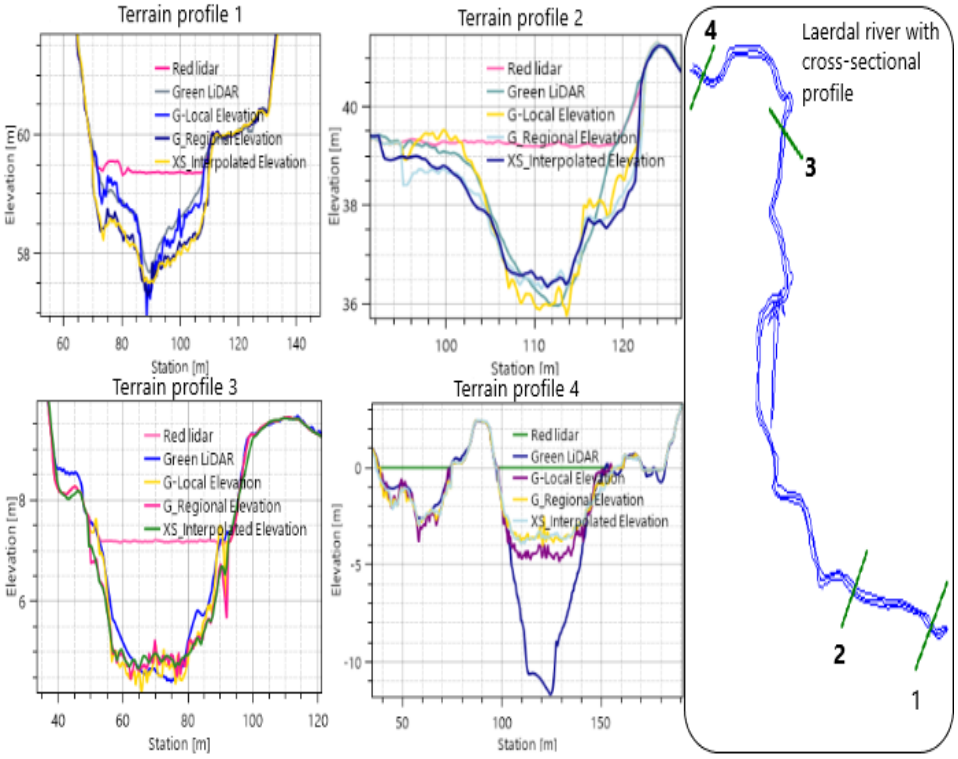

Figure 4.16: A comparison of the cross-sections of all of the derived Models with the Green and Red LiDAR data. The terrain profile of section 4 is taken toward to the sea and deeper than other sections.

demonstrate a good prediction of the observed Green-LiDAR depth. However, a slight overestimation and underestimation of the bathymetry observed in the profiles. The terrain profile from *section 4* [1] is taken toward the sea, and it is deeper than other sampled sections, both Local and Regional methods provide a good prediction for depths shallower than 5 m. Both methods are unable to provide reliable estimation of depths deeper than 5 m. However, Local method provides relatively better prediction of the depths deeper than 5 m. The results show that the Local method provides a good prediction for depths up to 5 m in deep and

[1] Section 4 is the section that is collected at the end of the lærdal river and it is a very deep section than other sections.

clear water, and the Regional method provides a good prediction for depths up to approximately 4 m. Note that Sundt et al. 2021 suggested a successful depth retrieval in river section with depth shallower than 2 m.

4.7 Hydraulic Simulation for Predicted and Lidar models

The hydraulic simulation was performed for the retrieved bathymetry (Local and Regional methods) as well as for the Red and Green Lidar bathymetric data. The model HEC-RAS was used for the simulation of inundation, and the simulation time was set to 16 hours for all flood flows. The normalized error was used to evaluate the quality of the prediction.

4.7.1 Minimum flood

A flood simulation for a minimum discharge of 10 m3/s was performed for predicted and Lidar models. The normalized error between the G-Local and the Green-Lidar is found to be B. The normalized error for the G-Regional method is shown in table 4.7. The normalized error shows a good fit with a slight overestimation of the flood with the observed bathyemtry. The normalized error for the Red lidar is found to be 1.39 showing an overestimation of the Green-lidar inundation.

4.7.2 Normal flood

Figure 4.17 displays the flood inundation of the mean discharge (QM) for the G-Regional and Lidar models. The G-Regional inundation is almost totally covered by the Green lidar inundation. On the other hand, the Red lidar inundated over a larger area than the G-Regional and the Green lidar. Table 4.7 shows the normalized error between predicted and observed bathymetry. The normalized error is found to be 0.94. This means that the predicted bathymetry corresponds very well with the observed. On the other hand, the normalized error for the Red-lidar is higher, suggesting an overestimation of the Green-Lidar.

4.7.3 High flood

The G-Local model shows a very good fit with the Green Lidar for the Q200 flood simulation (see table 4.7). The normalized error is found to be 1.09. This indicates that the Local method slightly underestimates the actual model for this flood scenario. The G-Regional model shows a good fit with the Green Lidar (see figure 4.18). The normalized error of the flooded area between G-Regional and Green lidar models is 0.79, indicating that the prediction is very good.

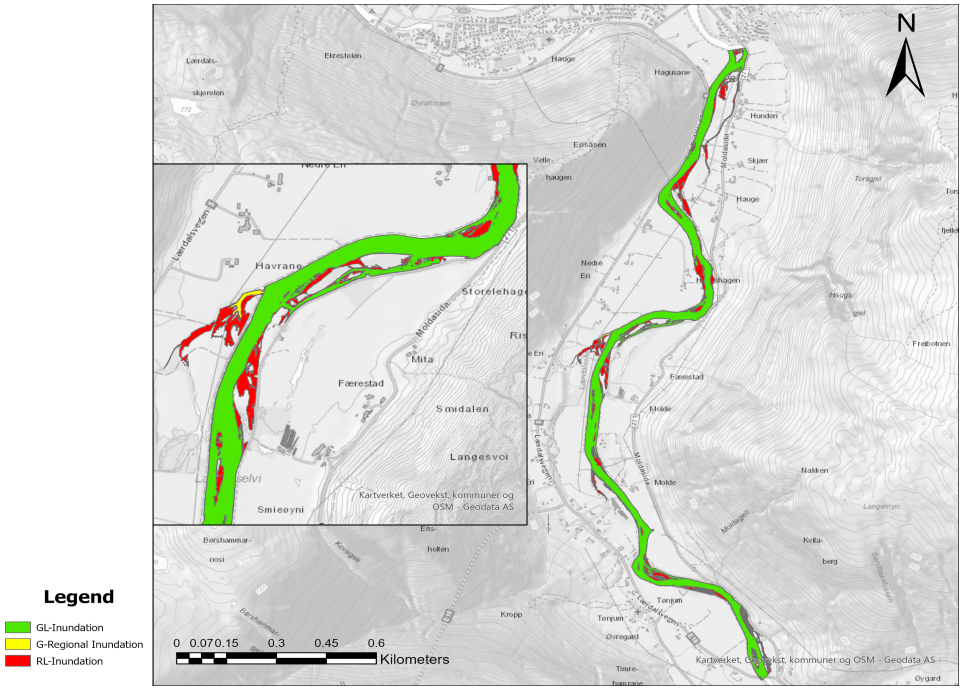

Figure 4.17: The extent of the flood inundation is displayed in ArcGIS after a QM flood simulation using HEC-RAS.

Figure 4.18 shows the flood inundation of Q200 for the Green and Red Lidars, and for the G-Regional and G-Local models. The Red-Lidar model shows higher inundation and covers a larger area of the flood plain than the other models. The normalized error for the Red-lidar is 1.7 (see table 4.7). This means that forecasting floods with the Red-Lidar results in a large overestimation of the actual flood inundation as expected.

Table 4.7: Normalized Error between predicted and Lidar models

Discharge (m3/s)	Normalized Error		
	RL	G-Regional	G-Local
Qmin (10m3/s)	1.39	1.12	1.09
QM	1.33	0.94	1.08
Q10	1.42	0.87	1.08
Q50	1.56	0.84	1.08
Q200	1.67	0.79	1.09

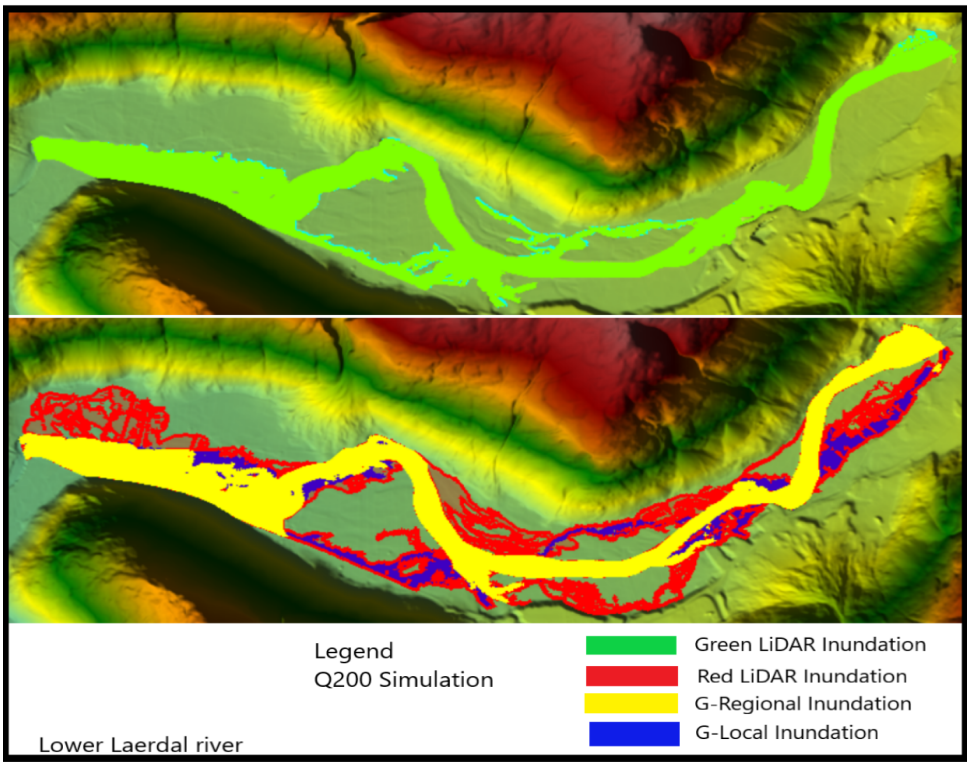

Figure 4.18: The Q200-years flood simulation by HEC-RAS. The extent of the flood inundation for Green Lidar (upper panel) and for predicted and Red Lidar (lower panel).

Chapter 5

Conclusion and Future Work

5.1 Conclusion

This study validates the the Regional method by using airborne scanned Green Lidar data from the Lærdal river. A local method was used to derive river bathymetry and then evaluate the quality of river depth retrieved by the Regional method. The Regional method was first introduced by Sundt et al. 2021 and was derived from four rivers located in the same region.

For both the Local and Regional methods, the Blue-band image-derived bathymetry has shown poor correspondence with the observed depth. whereas the Green-band has shown a good correspondence with the observed, with a slight overestimation of the depth. The local method provides better prediction compared to the regional method as expected. The regional method predicts river bathymetry up to 4 meters deep, whereas the local method predicts river bathymetry up to 5 meters deep depending on the clarity and substrates of the river.

The hydraulic simulation results showed that both the regional and local methods provide a good prediction for all flood flows considered in this thesis.

5.2 Future Works

For the present study, we attempted to remove artifacts manually using the ArcGIS tool, and classify the river area by creating classified polygons. This may lead to incorrect representation of the river bank due to vegetation shadow as well as fluvial deposits.

As a future work I recommend to develop an algorithm which is capable of treating vegetation shadows, fluvial deposits and other artifacts differently rather than removing part of the river.

Bibliography

Alne, I. S. (2016). *Topo-bathymetric lidar for hydraulic modeling-evaluation of lidar data from two rivers* (Master's thesis). NTNU.

Authority, T. N. M. (2022). Kartverket—terms of use. *Available online:www.kartverket.no/en/api-and-data/terms-of-use (accessed on 10 February 2022)*.

Awadallah, M. O. M., Juárez, A. & Alfredsen, K. (2022). Comparison between topographic and bathymetric lidar terrain models in flood inundation estimations. *Remote Sensing*, *14*(1), 227.

Breili, K., Simpson, M. J. R., Klokkervold, E. & Roaldsdotter Ravndal, O. (2020). High-accuracy coastal flood mapping for norway using lidar data. *Natural Hazards and Earth System Sciences*, *20*(2), 673–694.

Brunner, G. W. & Gibson, S. (2005). Sediment transport modeling in hec ras. *Impacts of global climate change* (pp. 1–12).

Bures, L., Roub, R., Sychova, P., Gdulova, K. & Doubalova, J. (2019). Comparison of bathymetric data sources used in hydraulic modelling of floods. *Journal of Flood Risk Management*, *12*, e12495.

Cobby, D. M., Mason, D. C. & Davenport, I. J. (2001). Image processing of airborne scanning laser altimetry data for improved river flood modelling. *ISPRS Journal of Photogrammetry and Remote Sensing*, *56*(2), 121–138.

Cook, A. & Merwade, V. (2009). Effect of topographic data, geometric configuration and modeling approach on flood inundation mapping. *Journal of hydrology*, *377*(1-2), 131–142.

Guenther, G. C., Brooks, M. W. & LaRocque, P. E. (2000). New capabilities of the "shoals" airborne lidar bathymeter. *Remote Sensing of Environment*, *73*(2), 247–255.

Holmqvist, E. (2000). Flomberegning for lærdalsvassdraget. *NVE: Oslo, Norway*.

Juárez, A., Alfredsen, K., Stickler, M., Adeva-Bustos, A., Suárez, R., Seguın-Garcıa, S. & Hansen, B. (2021). A conflict between traditional flood measures and maintaining river ecosystems? a case study based upon the river lærdal, norway. *Water*, *13*(14), 1884.

Jung, H. C., Jasinski, M., Kim, J.-W., Shum, C., Bates, P., Neal, J., Lee, H. & Alsdorf, D. (2012). Calibration of two-dimensional floodplain modeling in the central atchafalaya basin floodway system using sar interferometry. *Water Resources Research*, *48*(7).

Kinzel, P. J., Legleiter, C. J. & Nelson, J. M. (2013). Mapping river bathymetry with a small footprint green lidar: Applications and challenges 1. *JAWRA Journal of the American Water Resources Association*, *49*(1), 183–204.

Langsholt, E., Roald, L. A., Holmqvist, E. & Fleig, A. (2015). Flommen på vestlandet oktober 2014. *NVE rapport*, *11*, 2015.

Legleiter, C. J. & Harrison, L. R. (2019). Remote sensing of river bathymetry: Evaluating a range of sensors, platforms, and algorithms on the upper sacramento river, california, usa. *Water Resources Research*, *55*(3), 2142–2169.

Legleiter, C. J., Roberts, D. A. & Lawrence, R. L. (2009). Spectrally based remote sensing of river bathymetry. *Earth Surface Processes and Landforms*, *34*(8), 1039–1059.

Lejot, J., Delacourt, C., Piégay, H., Fournier, T., Trémélo, M.-L. & Allemand, P. (2007). Very high spatial resolution imagery for channel bathymetry and topography from an unmanned mapping controlled platform. *Earth Surface Processes and Landforms: The Journal of the British Geomorphological Research Group*, *32*(11), 1705–1725.

Lyon, J., Lunetta, R. & Williams, D. (1992). Airborne multispectral scanner data for evaluating bottom sediment types and water depths of the st. marys river, michigan. *Photogrammetric Engineering and Remote Sensing*, *58*(7), 951–956.

Lyzenga, D. R. (1978). Passive remote sensing techniques for mapping water depth and bottom features. *Applied optics*, *17*(3), 379–383.

Mandlburger, G., Hauer, C., Wieser, M. & Pfeifer, N. (2015). Topo-bathymetric lidar for monitoring river morphodynamics and instream habitats—a case study at the pielach river. *Remote Sensing*, *7*(5), 6160–6195.

Marcus, W. A., Legleiter, C. J., Aspinall, R. J., Boardman, J. W. & Crabtree, R. L. (2003). High spatial resolution hyperspectral mapping of in-stream habitats, depths, and woody debris in mountain streams. *Geomorphology*, *55*(1-4), 363–380.

Reil, A., Skoulikaris, C., Alexandridis, T. & Roub, R. (2018). Evaluation of riverbed representation methods for one-dimensional flood hydraulics model. *Journal of Flood Risk Management*, *11*(2), 169–179.

Stumpf, R. P., Holderied, K. & Sinclair, M. (2003). Determination of water depth with high-resolution satellite imagery over variable bottom types. *Limnology and Oceanography*, *48*(1part2), 547–556.

Sundt, H., Alfredsen, K. & Harby, A. (2021). Regionalized linear models for river depth retrieval using 3-band multispectral imagery and green lidar data. *Remote Sensing*, *13*(19), 3897.

Winterbottom, S. J. & Gilvear, D. J. (1997). Quantification of channel bed morphology in gravel-bed rivers using airborne multispectral imagery and aerial photography. *Regulated Rivers: Research & Management: An International Journal Devoted to River Research and Management*, *13*(6), 489–499.

Appendix A

Methods

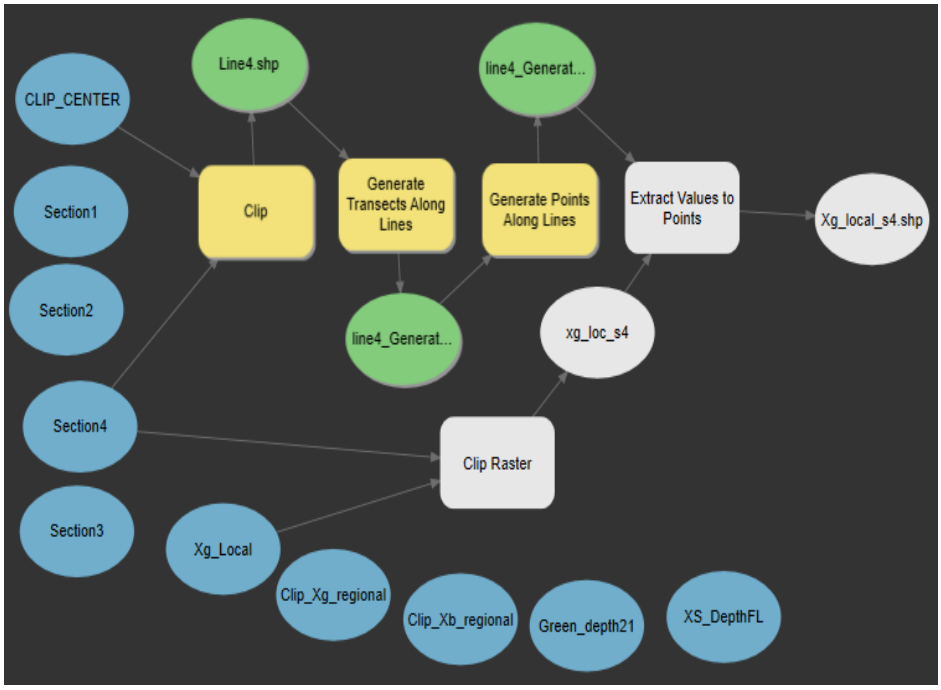

Figure A.1: Extracting point value from raster model as *.dbf file* using GiS-system

Appendix B

Result

B.1 Cross-sections and correlation coefficient values

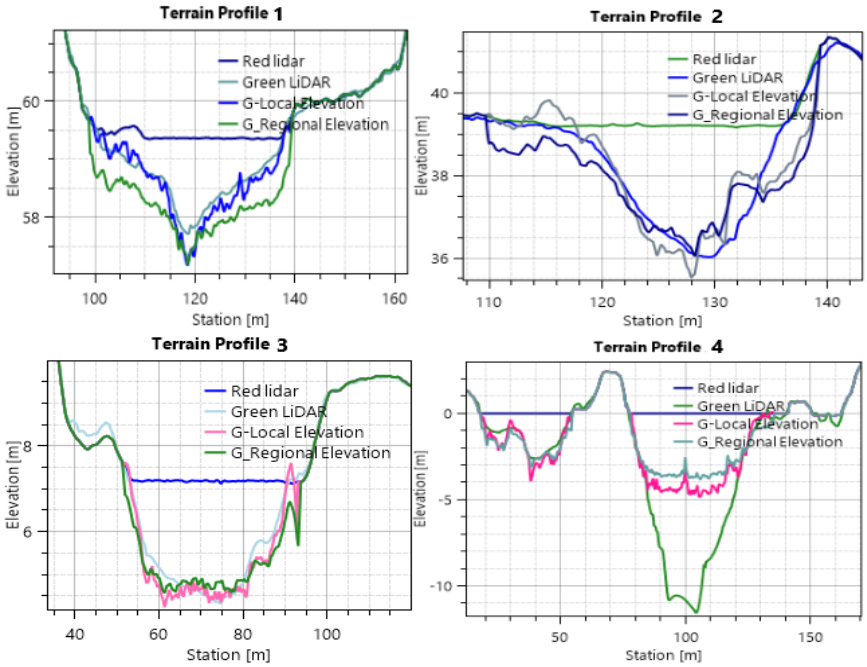

Figure B.1: Terrain profiles for Local and Regional models, as well at Red and LiDAR data.

B.2 Inundation of QM for predicted and Lidar models

Table B.1: The correlation of different image combinations and methods are displayed with coefficient's with regression fit R^2 and number of samples

Image band			Intercept			
Combination	RGB-Band	section	b0	b1	R2	n
Arial Imagery	G	1	0.30	4.15	0.54	72
		2	0.77	4.83	0.51	34
		3	0.32	5.93	0.69	92
		4	-0.82	12.06	0.76	208
		total section	-0.20	10.15	0.76	412
		full raster	0.39	6.63	0.65	225027
	B	1	0.54	0.98	0.05	72
		2	1.39	2.96	0.17	34
		3	1.51	1.83	0.10	92
		4	0.86	7.89	0.82	208
		total section	0.56	8.08	0.79	412
		full raster	1.10	1.39	0.05	225027
Local	B	1	O.098	0.30	0.38	213
		2	0.27	0.79	0.58	123
		3	0.07	0.81	0.58	236
		4	-0.40	1.45	0.81	425
		total section	-0.54	1.36	0.72	1003
		full raster	0.51	0.37	0.16	910987
	G	1	0.10	0.61	0.71	213
		2	0.26	0.85	0.86	123
		3	0.12	0.79	0.89	236
		4	-0.42	1.39	0.80	425
		total section	-0.27	1.26	0.82	1003
		full raster	0.34	0.78	0.57	910987
Regional	G	1	-0.50	0.89	0.67	212
		2	-0.63	1.28	0.85	125
		3	-0.72	1.21	0.88	236
		4	-1.90	2.13	0.80	422
		total section	-1.62	1.94	0.81	1001
		full raster	-0.43	1.16	0.58	983264
	B	1	0.11	0.41	0.35	212
		2	0.27	1.12	0.58	125
		3	0.03	1.19	0.56	236
		4	-0.46	2.14	0.83	422
		total section	-0.60	1.99	0.72	1001
		full raster	0.45	0.59	0.19	983264
XS Interpolated	G	1	-0.62	1.00	0.71	213
		2	-0.84	1.42	0.90	121
		3	-0.73	1.22	0.90	240
		4	-2.16	2.26	0.82	385

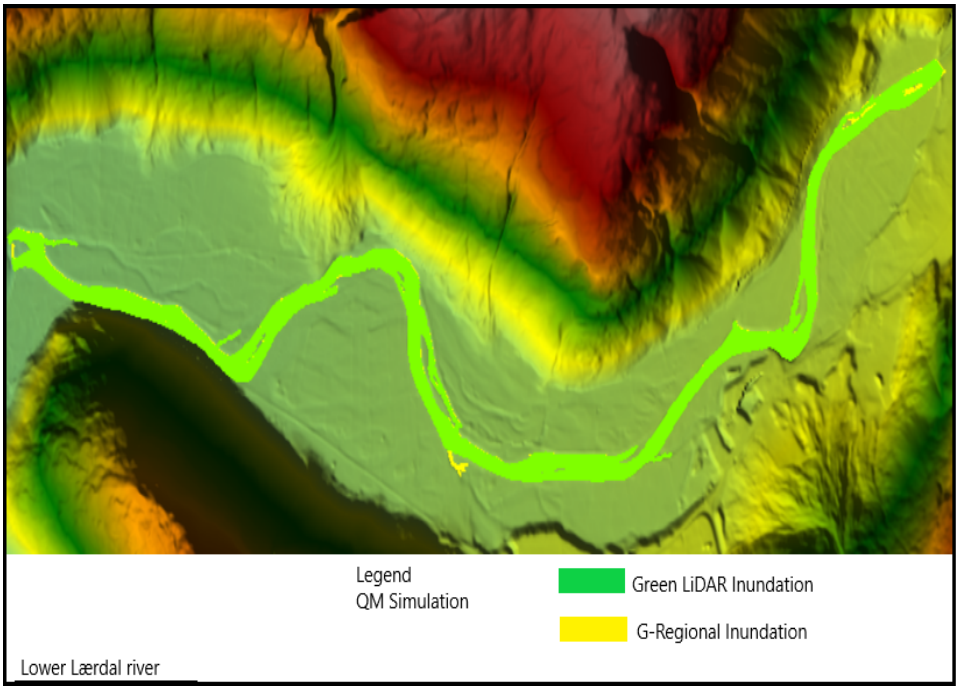

Figure B.2: Following a QM flood simulation with HEC-RAS, the comparison between G-Regional and Green LiDAR model using flood inundation. The G-Regional model has good fit with GL-model inundation.

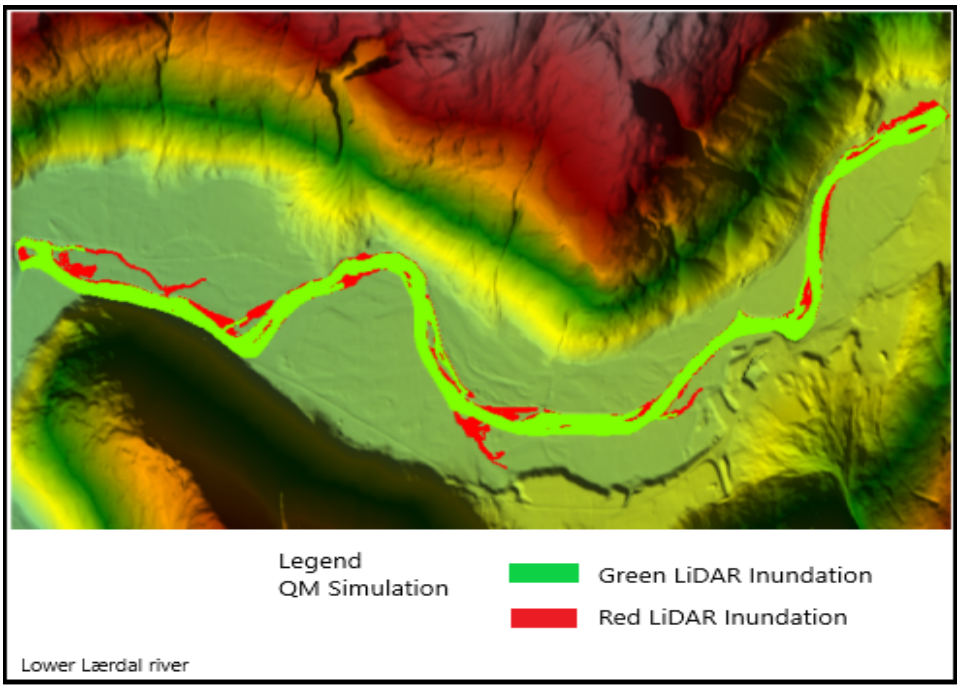

Figure B.3: QM flood simulation with HEC-RAS, the extent of the flood inundation comparison between RED AND GREEN LiDAR MODEL. RED LiDAR inundates more flood plain area.

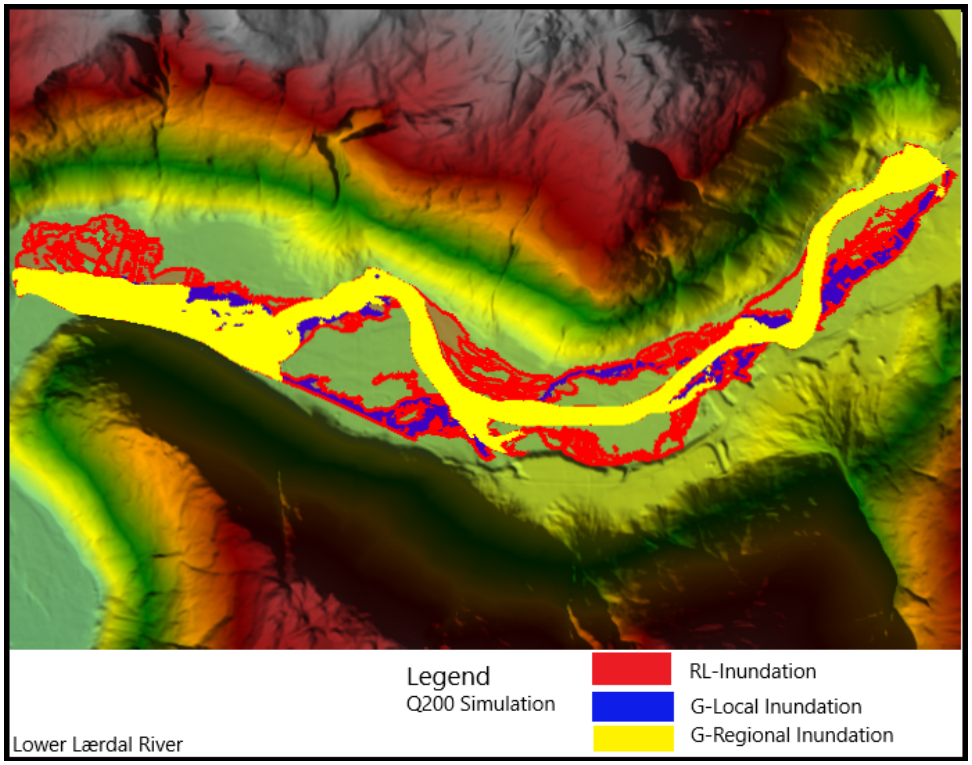

Figure B.4: Q200-year flood simulation using HEC-RAS, The extent of the flood's inundation for all predicted and Red LiDAR model.